Article

Aryl-Substituted C-Bridged Oligopyrroles as Anion Receptors for Formation of Supramolecular Organogels

Hiromitsu Maeda, Yohei Haketa, and Takashi Nakanishi

J. Am. Chem. Soc., **2007**, 129 (44), 13661-13674• DOI: 10.1021/ja074435z • Publication Date (Web): 10 October 2007

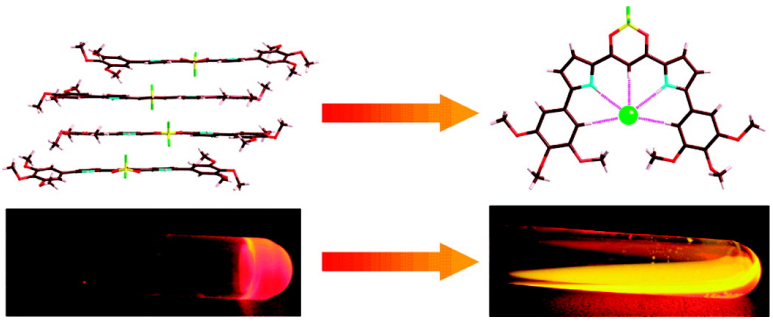

J|A|C|S
ARTICLES
Published on Web 10/10/2007

Aryl-Substituted C_3-Bridged Oligopyrroles as Anion Receptors for Formation of Supramolecular Organogels

Hiromitsu Maeda,[†,‡,*] Yohei Haketa,[†] and Takashi Nakanishi[§,||]

Contribution from the Department of Bioscience and Biotechnology, Faculty of Science and Engineering, Ritsumeikan University, Kusatsu 525-8577, Japan, Department of Materials Molecular Science, Institute for Molecular Science (IMS), Okazaki 444-8787, Japan, Organic Nanomaterials Center, National Institute for Materials Science (NIMS), Tsukuba 305-0047, Japan, and MPI-NIMS International Joint Laboratory, Max Planck Institute of Colloids and Interfaces, 14424 Potsdam, Germany

Received June 18, 2007; E-mail: maedahir@se.ritsumei.ac.jp

Abstract: BF_2 complexes of aryl-substituted dipyrrolyldiketones (**3a**−**c**, **5a**−**d**) have been synthesized by the condensation of arylpyrroles obtained by Suzuki cross-coupling reactions with malonyl chloride, followed by treatment with BF_3·OEt_2. The binding constants (K_{a11}) of the BF_2 complexes (**3a**−**c**) for various anions (Cl^-, Br^-, $CH_3CO_2^-$, $H_2PO_4^-$, and HSO_4^-) in CH_2Cl_2 decrease in the order Ph (**3a**) > *o*-tolyl (**3b**) > 2,6-Me_2Ph (**3c**), possibly because of differences in the planarity and the number of interacting *o*-CH units at the binding sites. Aryl-substituted receptors exhibit a [1+1] binding mode with Cl^- as well as a [2+1] binding mode under conditions of high concentration and low temperature, as suggested by ^{1}H NMR studies in CD_2Cl_2. These receptors, especially phenyl-substituted (**3a**) and *o*-tolyl (**3b**), exhibit drastic colorimetric and fluorescent changes in the presence of F^- due to extended π-conjugation, as compared to 2,6-dimethylphenyl (**3c**) and the previously reported derivatives (**1a**−**c**). Aryl-substitution at the α-positions of pyrrole is an excellent means for the introduction of various substituents at the periphery of the anion receptors. For example, derivatives with long alkoxy chains at 3,4,5-positions of the substituent aryl rings (**5b**−**d**) afford emissive gel structures in hydrocarbon solvents, such as octane, based on the stacking of slipped *H*- and *J*-aggregates at the core π-plane. The structural organization of the supramolecular gels was investigated by AFM, SEM, and XRD measurements as well as by considering the solid-state packing of crystalline derivatives. The slow transformation of the gel to the solution phase by the addition of various anions, possibly except for F^-, is correlated with the unique properties of these acyclic receptors where inversions of pyrrole rings are required for anion binding. Boron complexes of 1,3-dipyrrolyl-1,3-propanediones with aryl-substituents, as a new class of acyclic anion receptors, have shown efficient binding due to the interacting *o*-CH units and, in the case of the derivative with long aliphatic chains, afforded the emissive supramolecular organogels using stacking of core π-planes controlled by external chemical stimuli.

Introduction

π-Conjugated oligomers that are capable of guest binding are fascinating and potentially useful materials because of the possible solvent-free detection of analytes in the solid (i.e., film) state.[1] One of the many advantages of receptors based on π-conjugated oligomers over small molecules is their potential to provide amplified properties that are sensitive to subtle perturbations by the guest species. Therefore, dynamic conformational changes in oligomeric systems through guest recognition should also be useful for the organization and modulation of the associated structures.[2−4] Apart from the ordinary "covalently" linked oligomers, supramolecular assemblies assisted by noncovalent interactions such as hydrogen bonding and van der Waals interactions can be considered as "stacking" oligomers. Among the self-assembled oligomeric systems based on

† Ritsumeikan University.
‡ Institute for Molecular Science.
§ National Institute for Materials Science.
|| Max Planck Institute of Colloids and Interfaces.

(1) (a) Swager, T. M. In *Acetylene Chemistry*; Diederich, F., Stang, P. J., Tykwinski, R. R., Eds.; Wiley−VCH: New York, 2005; Chapter 6. (b) McQuade, D. T.; Pullen, A. E.; Swager, T. M. *Chem. Rev.* **2000**, *100*, 2537−2574. (c) Rose, A.; Shu, Z.; Madigan, C. F.; Swager, T. M.; Bulović, V. *Nature* **2005**, *434*, 876−879.

(2) (a) Prince, R. B.; Okada, T.; Moore, J. S. *Angew. Chem., Int. Ed.* **1999**, *38*, 233−236. (b) Prince, R. B.; Barnes, S. A.; Moore, J. S. *J. Am. Chem. Soc.* **2000**, *122*, 2758−2762. (c) Tanatani, A.; Mio, M. J.; Moore, J. S. *J. Am. Chem. Soc.* **2001**, *123*, 1792−1793. (d) Tanatani, A.; Hughes, T. S.; Moore, J. S. *Angew. Chem., Int. Ed.* **2002**, *41*, 325−328. (e) Nishinaga, T.; Tanatani, A.; Oh, K.; Moore, J. S. *J. Am. Chem. Soc.* **2002**, *124*, 5934−5935.

(3) (a) Yashima, E.; Maeda, K.; Nishimura, T. *Chem. Eur. J.* **2004**, *10*, 42−51. (b) Maeda, K.; Takeyama, Y.; Sakajiri, K.; Yashima, E. *J. Am. Chem. Soc.* **2004**, *126*, 16284−16285. (c) Miyagawa, T.; Furuko, A.; Maeda, K.; Katagiri, H.; Furusho, Y.; Yashima, E. *J. Am. Chem. Soc.* **2005**, *127*, 5018−5019. (d) Nagai, K.; Maeda, K.; Takeyama, Y.; Sakajiri, K.; Yashima, E. *Macromolecules* **2005**, *38*, 5444−5451. (e) Onouchi, H.; Hasegawa, T.; Kashiwagi, D.; Ishiguro, H.; Maeda, K.; Yashima, E. *Macromolecules* **2005**, *38*, 8625−8633. (f) Onouchi, H.; Miyagawa, T.; Morino, K.; Yashima, E. *Angew. Chem., Int. Ed.* **2006**, *45*, 2381−2384. (g) Hasegawa, T.; Morino, K.; Tanaka, Y.; Katagiri, H.; Furusho, Y.; Yashima, E. *Macromolecules* **2006**, *39*, 482−488.

(4) (a) Inouye, M.; Waki, H.; Abe, H. *J. Am. Chem. Soc.* **2004**, *126*, 2022−2027. (b) Abe, H.; Masuda, N.; Waki, M.; Inouye, M. *J. Am. Chem. Soc.* **2005**, *127*, 16189−16196.

low-molecular weight π-conjugated molecules, the gel materials, especially those susceptible to influence by external stimuli, are of interest and play a crucial role as functional soft materials.[5−7] For example, Shinkai et al. have reported the properties of thixotropy and mixed valence state unique in an organogel, controlled by mechanical and electrochemical stimuli and based on the π-conjugated porphyrin and TTF moieties, respectively.[6] On the other hand, Yagai et al. have fabricated photoresponsive organogels consisting of hydrogen-bonded aggregates of melamine−azobenzene conjugates and their complementary units.[7] In contrast to the available physical stimuli, the chemically controlled structural modification of supramolecular organogels is very attractive since a huge variety of potential additives are available.[8]

Among the various available stimuli or "targets" to regulate the structures of π-conjugated oligomers and their assembled forms, inorganic and biotic anions such as halides, acetates, and phosphates, ubiquitous in biology, are essential as seen in the activity of enzymes, transport of hormones, protein synthesis, and DNA regulation.[9,10] Compared with the cyclic anion receptors with preorganized structures, the acyclic ones are required to dynamically change their conformations for binding.[11−13] Previously, we have synthesized the BF_2 complexes of 1,3-dipyrrolyl-1,3-propanediones (e.g., **1a**−**c**) with planar structures, and these efficient acyclic anion receptors use NH and bridging CH sites with the inversion of two pyrrole rings (Scheme 1).[14] Substitution of aryl rings at the extremes of the receptor units could yield various functional derivatives, depending on the substituents; these π-extended systems can also be used as scaffolds for the fabrication of covalent and noncovalent oligomers possessing anion-binding capabilities. Furthermore, aryl moieties might enable a facile chromogenic detection of anions and thus act as effective anion sensors. In this article, we report the synthesis and anion-binding properties of the BF_2 complexes of aryl-substituted dipyrrolyldiketones. Some derivatives show augmented affinities for anions because of the additional sp^2 *o*-CH positions, which act as interacting positions at the tethered aryl groups. Multipoint interactions by acyclic receptors afford various anion-binding modes and stoichiometries according to the conditions. Furthermore, in these acyclic systems, gel formation, which can be controlled by the addition of anions, has been observed in the derivatives with long peripheral aliphatic chains.

Scheme 1. Anion Binding of Acyclic Anion Receptors **1a**−**c**

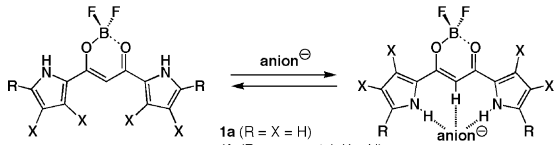

Results and Discussion

Synthesis and Characterization of Aryl-Substituted C_3-Bridged Oligopyrroles. α-Aryl-substituted diketones **2a**−**c** were obtained in 45, 46, and 69% yields, respectively, from the corresponding arylpyrroles and malonyl chloride in CH_2Cl_2.[15,16] Subsequent complexation using $BF_3{\cdot}OEt_2$ afforded highly fluorescent BF_2 complexes **3a**−**c** in 97, 84, and 78% yields, respectively. The starting arylpyrroles were synthesized by Suzuki cross-coupling reactions of *N*-BOC-pyrrole boronic acid and the corresponding arylbromides, followed by deprotection by heating in ethylene glycol (Scheme 2).[17] The initial characterization of **3a**−**c** was performed by NMR and FAB-MS. The absorption maxima (λ_{max}) of **3a**,**b** in CH_2Cl_2 appear at 500 and 480 nm, respectively, which are red-shifted compared to the unsubstituted **1a** (432 nm) and α-neopentyl **1b** (457 nm) because of the π-conjugated aryl units. Conversely, as a result of distortion of the aryl rings the λ_{max} for **3c** appears at 456 nm, blue-shifted by 44 and 24 nm compared with **3a** and **3b**, respectively.

Single-crystal X-ray diffraction analyses of **3a**−**c** are shown in Figure 1a(i−iii). The dihedral angles subtended by the slightly distorted aryl substituents to the dipyrrolyl core plane consisting of 16 atoms are 20.0° and 28.6° for **3a**, 1.8° and 38.0° (26.1° and 23.3° (disordered), and 38.2° in the other independent molecule) for **3b**, and more closely approach perpendicularity

(5) (a) *Low Molecular Mass Gelators*; Fages, F., Ed.; *Topics in Current Chemistry*; Springer-Verlag: Berlin, 2005; Vol. 256, pp 283. (b) Ishi-i, T.; Shinkai, S. In *Supramolecular Dye Chemistry*; Würthner, F., Ed.; *Topics in Current Chemistry*; Springer-Verlag: Berlin, 2005; Vol. 258, pp 119−160. (c) Terech, P.; Weiss, R. G. *Chem. Rev.* **1997**, *97*, 3133−3159. (d) Abdallah. D. J.; Weiss, R. G. *Adv. Mater.* **2000**, *12*, 1237−1247. (e) van Esch, J. H.; Feringa, B. L. *Angew. Chem., Int. Ed.* **2000**, *39*, 2263−2266.
(6) (a) Shirakawa, M.; Fujita, N.; Shinkai, S. *J. Am. Chem. Soc.* **2005**, *127*, 4164−4165. (b) Kitahara, T.; Shirakawa, M.; Kawano, S.-i.; Beginn, U.; Fujita, N.; Shinkai, S. *J. Am. Chem. Soc.* **2005**, *127*, 14980−14981.
(7) Yagai, S.; Nakajima, T.; Kishikawa, K.; Kohmoto, S.; Karatsu, T.; Kitamura, A. *J. Am. Chem. Soc.* **2005**, *127*, 11134−11139.
(8) (a) Sugiyasu, K.; Fujita, N.; Takeuchi, M.; Yamada, S.; Shinkai, S. *Org. Biomol. Chem.* **2003**, *1*, 895−899. (b) Zang, Y.; Gu, H.; Yang, Z.; Xu, B. *J. Am. Chem. Soc.* **2003**, *125*, 13680−13681. (c) Sreenivasachary, N.; Lehn, J.-M. *Proc. Nat. Acad. Sci. U.S.A.* **2005**, *102*, 5938−5943. (d) Varghese, R.; George, S. J.; Ajayaghosh, A. *Chem. Commun.* **2005**, 593−595. (e) Ghoussoub, A.; Lehn, J.-M. *Chem. Commun.* **2005**, 5763−5765. (f) Stanley, C. E.; Clarke. N.; Anderson, K. M.; Elder, J. A.; Lenthall, J. T.; Steed, J. W. *Chem. Commun.* **2006**, 3199−3201. (g) Wang, C.; Zhang, D.; Zhu, D. *Langmuir* **2007**, *23*, 1478−1482. (h) Li, Q.; Wang, Y.; Li, W.; Wu, L. *Langmuir* **2007**, *23*, 8217−8223. (i) Yang, H.; Yi, T.; Zhou, Z.; Zhou, Y.; Wu, J.; Xu, M.; Li, F.; Huang, C. *Langmuir* **2007**, *23*, 8224−8230.
(9) (a) Bianchi, A., Bowman-James, K., García-España, E., Eds. *Supramolecular Chemistry of Anions*; Wiley-VCH: New York, 1997. (b) Singh, R. P.; Moyer, B. A. Eds. *Fundamentals and Applications of Anion Separations*; Kluwer Academic/Plenum Publishers: New York, 2004. (c) Stibor, I., Ed. *Anion Sensing*; *Topics in Current Chemistry*; Springer-Verlag: Berlin, 2005; Vol. 255, pp 238. (d) Sessler, J. L.; Gale, P. A.; Cho, W.-S. *Anion Receptor Chemistry*; Royal Society of Chemistry: Cambridge, 2006.
(10) (a) Schmidtchen, F. P.; Berger, M. *Chem. Rev.* **1997**, *97*, 1609−1646. (b) Beer, P. D.; Gale, P. A. *Angew. Chem., Int. Ed.* **2001**, *40*, 487−516. (c) Martínez-Mãnez, R.; Sancenón, F. *Chem. Rev.* **2003**, *103*, 4419−4476. (d) Gale, P. A.; Quesada, R. *Coord. Chem. Rev.* **2006**, *250*, 3219−3244.
(11) Gale, P. A. *Acc. Chem. Res.* **2006**, *39*, 465−475.
(12) (a) Kavallieratos, K.; de Gala, S. R.; Austin, D. J.; Crabtree, R. H. *J. Am. Chem. Soc.* **1997**, *119*, 2325−2326. (b) Kavallieratos, K.; Bertao, C. M.; Crabtree, R. H. *J. Org. Chem.* **1999**, *64*, 1675−1683.
(13) (a) Black, C. B.; Andrioletti, B.; Try, A. C.; Ruiperez, C.; Sessler, J. L. *J. Am. Chem. Soc.* **1999**, *121*, 10438−10439. (b) Anzenbacher, P., Jr.; Try, A. C.; Miyaji, H.; Jursikova, K.; Lynch, V. M.; Marquez, M.; Sessler, J. L. *J. Am. Chem. Soc.* **2000**, *122*, 10268−10272. (c) Mizuno, T.; Wei, W.-H.; Eller, L. R.; Sessler, J. L. *J. Am. Chem. Soc.* **2002**, *124*, 1134−1135. (d) Sessler, J. L.; Maeda, H.; Mizuno, T.; Lynch, V. M.; Furuta, H. *Chem. Commun.* **2002**, 862−863. (e) Sessler, J. L.; Pantos, G. D.; Katayev, E.; Lynch, V. M. *Org. Lett.* **2003**, *5*, 4141−4144. (f) Coles, S. J.; Frey, J. G.; Gale, P. A.; Hursthouse, M. B.; Light, M. E.; Navakhun, K.; Thomas, G. L. *Chem. Commun.* **2003**, 568−569. (g) Vega, I. E. D.; Gale, P. A.; Hursthouse, M. B.; Light, M. E. *Org. Biomol. Chem.* **2004**, *2*, 2935−2941. (h) Sessler, J. L.; Pantos, G. D.; Gale, P. A.; Lynch, V. M. *Org. Lett.* **2006**, *8*, 1593−1596. (i) Sessler, J. L.; Cho, D.-G.; Lynch, V. M. *J. Am. Chem. Soc.* **2006**, *128*, 16518−16519.
(14) (a) Maeda H.; Kusunose, Y. *Chem. Eur. J.* **2005**, *11*, 5661−5666. (b) Fujimoto, C.; Kusunose, Y.; Maeda, H. *J. Org. Chem.* **2006**, *71*, 2389−2394. (c) Maeda, H.; Ito, Y. *Inorg. Chem.* **2006**, *45*, 8205−8210. (d) Maeda, H.; Ito, Y.; Kusunose, Y. *Chem. Commun.* **2007**, 1136−1138. (e) Maeda, H.; Kusunose, Y.; Terasaki, M.; Ito, Y.; Fujimoto, C.; Fujii, R.; Nakanishi, T. *Chem. Asian J.* **2007**, *2*, 350−357. (f) Maeda, H.; Kusunose, Y.; Mihashi, Y.; Mizoguchi, T. *J. Org. Chem.* **2007**, *72*, 2612−2616.
(15) Oddo, B.; Dainotti, C. *Gazz. Chim. Ital.* **1912**, *42*, 716−726.
(16) Stark, W. M.; Baker, M. G.; Leeper, F. J.; Raithby, P. R.; Battersby, A. R. *J. Chem. Soc., Perkin Trans. 1* **1988**, 1187−1201.
(17) (a) Johnson, C. N.; Stemp, G.; Anand, N.; Stephen, S. C.; Gallagher, T. *Synlett* **1998**, 1025−1027. (b) Burghart, A.; Kim, H.; Welch, M. B.; Thoresen, L. H.; Reibenspies, J.; Burgess, K. *J. Org. Chem.* **1999**, *64*, 7813−7819.

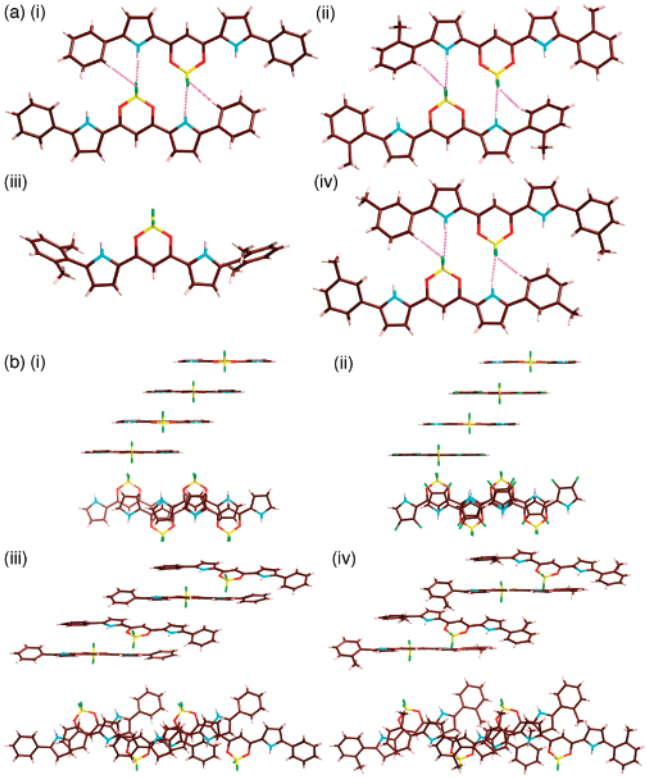

Figure 1. (a) Single-crystal X-ray structures of (i) **3a**, (ii) **3b** (one of the three conformations), (iii) **3c** (one of the two conformations), and (iv) **3b′** as dimeric assemblies except for **3c**. (b) Stacking structures (side and top views) of (i) **1a**, (ii) **1c**, (iii) **3a**, and (iv) **3b** in the solid state. Atom color code: brown, pink, yellow, green, blue, and red refer to carbon, hydrogen, boron, fluorine, nitrogen, and oxygen, respectively.

Scheme 2. Synthesis of **3a**−**c**

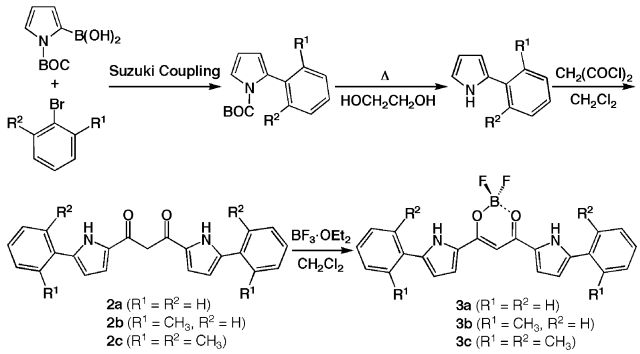

at 70.8° and 71.2° (75.8° and 87.8° in the other form) for **3c**. In the solid state, one of the tolyl-methyl units of **3b** is oriented toward the NH site of pyrrole in the disordered structure. The blue-shifted absorption maxima of **3b** and **3c** relative to that of **3a** are consistent with the small disruption of the π-conjugation due to a larger relative distortion than those of **3a** and *m*-tolyl derivative **3b′** (21.0° and 23.8°, Figure 1a(iv), $\lambda_{max} = 502$ nm in CH_2Cl_2), also supported by theoretical studies (vide infra). Further, **3a** as well as **3b** and **3b′** forms a dimeric structure, wherein the *o*-C(−H)···F distance is 3.35 Å compared with 3.13 and 3.16 Å for N(−H)···F, while such dimeric assemblies are not formed for **3c**. Thus, the weak interaction of *o*-CH should play the role of a ligand for the anions in solution. Aryl substitution at the α-positions of pyrrole also affects the stacking structures in the solid state (Figure 1b). Similar to the α-unsubstituted **1a**,**c** which exhibits the slipped $\pi-\pi$ stacking

Table 1. Binding Constants (K_{a11}, M^{-1}) of Aryl-Substituted BF_2 Complexes **3a**−**c** and α-Alkyl **1b** as a Reference Receptor with Various Anions in CH_2Cl_2[a,b]

	K_{a11}(**3a**)	K_{a11}(**3b**)	K_{a11}(**3c**)	K_{a11}(**1b**)
F^-	240,000 (3.0)	170,000 (2.1)	180,000 (2.2)	81,000 [c]
Cl^-	30,000 (15)	2,500 (1.3)	1,000 (0.50)	2,000 [c]
Br^-	2,800 (8.5)	300 (0.91)	150 (0.45)	330 [c]
$CH_3CO_2^-$	210,000 (1.9)	150,000 (1.4)	71,000 (0.65)	110,000 [d]
$H_2PO_4^-$	72,000 (5.5)	8,000 (0.62)	1,400 (0.11)	13,000 [c]
HSO_4^-	540 (6.8)	35 (0.44)	14 (0.18)	80 [c]

[a] The values in the parentheses are the ratios to K_{a11} of **1b**. [b] The errors of K_{a11} for F^- and other anions are within 20 and 13%, respectively, as seen in the Supporting Information. [c] Reference 14a. [d] Reference 14c.

structures with interplane distances of 3.311−3.352 and 3.455−3.458 Å, respectively (Figure 1b(i,ii)), stacking assemblies are also observed in the crystal of aryl-substituted **3a**,**b** (Figure 1b-(iii,iv)), wherein the distance between the plane of the core 16 atoms and the phenylpyrrole unit of the neighboring molecule in **3a** is 3.190−3.873 Å. Here, the slightly distorted aryl rings in **3a** and **3b** afford a less effective stacking. In contrast, **3c** shows a stacking between the aryl ring and the core π-plane but no interactions between the dipyrrolyldiketone moieties. The solid-state assemblies seen in **1a**,**c** and **3a**,**b** can be correlated with the supramolecular structures as described in the following section.

Anion-Binding Studies by Changes in the UV/Vis Absorption Spectra. The anion affinities of the aryl-substituted receptors were estimated from the changes in the UV/vis absorption spectra in the presence of increasing concentrations of the respective anions. The absorption maxima of **3a**−**c** persist at 501, 483, and 459 nm with new shoulders in the long-wavelength region upon the addition of F^- as its tetrabutylammonium (TBA) salt in CH_2Cl_2. Greater excesses of F^- gave rise to new bands at 536 (**3a**), 523 (**3b**), and 462 and 484 nm (**3c**), which were possibly derived from the deprotonated species.[18] On the other hand, the λ_{max} values were hardly affected (ca. 2−5 nm) by binding with other anions such as Cl^-, and the intensity was moderately decreased. The association constants (K_{a11}) of **3a**−**c**, estimated from the changes in the absorption spectra, are summarized in Table 1. Compared to α-alkyl-substituted **1b**, α-phenyl **3a** shows augmented K_{a11}, especially for Cl^- (ca. 15-fold enhancement). The binding stoichiometry (1:1) was determined by Job plots using **3a** and Cl^-. In contrast, the doubly *o*-C-blocked **3b** exhibits lesser K_{a11} than those of **3a** and are comparable to those of **1b**. Further, the completely *o*-C-blocked **3c** shows a lower K_{a11} (ca. 1/2) than **3b**. This is possibly due to steric hindrance as well as the electrostatic repulsion of the anions by the π-plane and an entropy loss due to the distortion of the 2,6-dimethylphenyl

(18) (a) Possible deprotonated species could be stabilized by intramolecular hydrogen bonding between *o*-CH and pyrrole N. ESI-TOF-MS (ref 21) also excludes the formation of [1+2 (= receptor + F^-)] binding. (b) Camiolo, S.; Gale, P. A.; Hursthouse, M. B.; Light, M. E.; Shi, A. J. *Chem. Commun.* **2002**, 758−759. (c) Gale, P. A.; Navakhun, K.; Camiolo, S.; Light, M. E.; Hursthouse, M. B. *J. Am. Chem. Soc.* **2002**, *124*, 11228−11229. (d) Amendola, V.; Esteban-Goméz, D.; Fabbrizzi, L.; Licchelli, M. *Acc. Chem. Res.* **2006**, *39*, 343−353. (e) Wu, C.-Y.; Chen, M.-S.; Lin, C.-A.; Lin, S.-C.; Sun, S.-S. *Chem. Eur. J.* **2006**, *12*, 2263−2269.

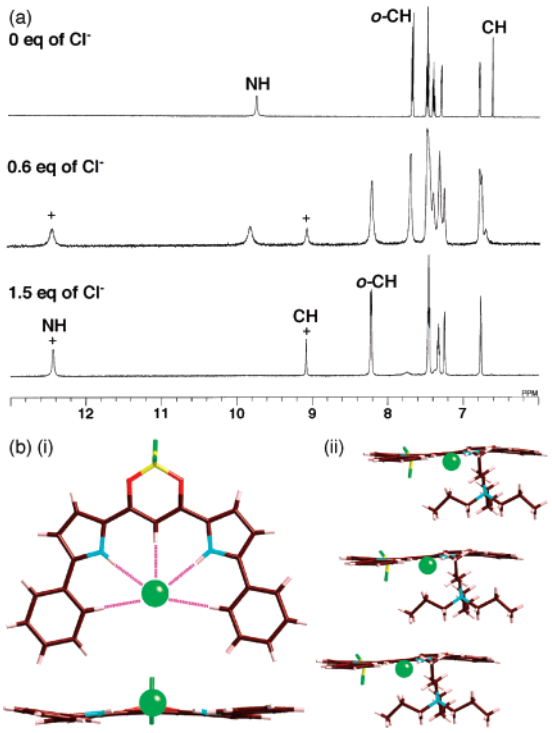

Figure 2. (a) ^{1}H NMR spectral changes of **3a** in CD_2Cl_2 at 20 °C upon the addition of Cl^- as a TBA salt (the signals of [1+1] complexes are labeled by plus marks). (b) (i) Single-crystal X-ray structure (top and side views) of Cl^- complex of **3a** and (ii) columnar structure. Solvents are omitted for clarity.

moieties. Other possible factors may be the weak but rather effective interaction by the sp^2 CH moieties as compared with the sp^3 CH moieties of the side chains (methyl moieties in this case). For the difference between **3a** and **3b**, the "probability" factor due to the numbers of *o*-CH (*four* for **3a** and *two* for **3b**) may also be crucial.

Multiple Cl^- Binding Modes Observed by ^{1}H NMR, X-ray Analysis, ESI-MS, and DFT Studies. Of the various anion receptors reported so far, the rigid cyclic triamide derivatives have shown various binding modes and stoichiometries, monitored by ^{1}H NMR, depending on the association conditions.[19] Similarly, the changes in ^{1}H NMR spectra of the aryl-substituted derivatives **3a**−**c** by anions such as Cl^- as the representative in CD_2Cl_2 provided valuable insights such as (a) the binding behaviors of *o*-CH as well as pyrrole NH and bridging CH and (b) the possible binding modes.

Upon the addition of 1.5 equiv of Cl^- to a CD_2Cl_2 solution of **3a** (1×10^{-3} M) at 20 °C, the signals due to **3a** at 7.68 (*o*-CH), 9.73 (pyrrole NH), and 6.23 (bridging CH) ppm decreased in intensity with the concurrent appearance of new signals at 8.19, 12.27, and 9.04 ppm, respectively (Figure 2a). The peak derived from the *o*-CH of the Cl^- complex (**3a**·Cl^-) with the integration of 4H in the downfield region suggests (i) an interaction between the *o*-CH and the anion and (ii) a rather rapid exchange (free rotation) between the anion-binding *o*-CH and "anion-free" *o*-CH at this temperature. Further, the signals due to the receptor **3a** and the complex **3a**·Cl^- can be observed independently as also seen in the derivatives such as **1b**,**c**,[14a,c] which suggests a slow exchange between these species on the NMR time scale. Furthermore, X-ray analysis of the anion complex **3a**·Cl^- (Figure 2b) suggests a pentacoordinated geometry of the [1+1] complex with the distances of 3.261−3.319 Å (N(−H)···Cl), 3.403 and 3.382 Å (C(−H)···Cl), and 3.592−3.613 Å (*o*-C(−H)···Cl). The dihedral angles between the aryl rings and the core planes are estimated as 6.1° and 9.5°, which are smaller than those of anion-free **3a**; this suggests that a greater planarity can be achieved from a "less-planar" flexible acyclic geometry by means of anion binding. The formation of a π-stacking and an electrostatically mediated columnar structure consisting of a **3a**·Cl^- plane and a tetrapropylammonium (TPA) cation is also observed in the solid state.

Similar trends in the downfield shifts of the pyrrole NH and the bridging CH have also been observed in the other aryl-substituted receptors **3b**,**c** (1×10^{-3} M) at 20 °C (see the Supporting Information). In the case of *o*-tolyl-substituted **3b**, the corresponding signals at 9.56 (NH) and 6.64 (CH) ppm diminished and are detected as new peaks at 12.31 and 9.04 ppm, respectively, upon the addition of Cl^- (5 equiv). Similar to the case of **3a**, the *o*-CH signal at 7.46 ppm is shifted to 7.86 ppm. The shift differences between the free receptor and the complex ($\Delta\delta$) are estimated to be 0.51 (*o*-CH), 2.54 (NH), and 2.81 (bridging CH) ppm for **3a** and 0.40 (*o*-CH), 2.75 (NH), and 2.40 (bridging CH) ppm for **3b**. The smaller *o*-CH $\Delta\delta$ value for **3b** relative to that of **3a**, being the average shift between the binding *o*-CH and free *o*-CH in **3a**·Cl^-, could also be derived from the slight distortion of the aryl rings in **3b**. On the other hand, in 2,6-dimethylphenyl **3c**, wherein the NH and the bridging CH peaks are observed at 9.37 and 6.63 ppm, the $\Delta\delta$ values are 2.77 and 2.21 ppm, respectively, in the presence of Cl^- (5 equiv). The other signals in **3a**−**c**, such as pyrrole β-CH and *m*- and *p*-ArH, exhibit slightly upfield shifts, for example, one of the β-CH signals of **3a** is shifted from 6.80 to 6.77 ppm due to the shielding effect caused by the negatively charged species.

^{1}H NMR spectral changes of **3a**−**c** (1×10^{-3} M) upon Cl^- binding at −50 °C in CD_2Cl_2 show similar trends as seen at 20 °C, and new signals are observed (see the Supporting Information).[20] At −50 °C, the new NH signals appear at 11.55 (**3a**), 11.22 (**3b**), and 10.72 (**3c**) ppm with small amounts of Cl^- (0.6, 1.0, and 1.0 equiv for **3a**−**c**, respectively). Upon increasing the anion concentration, these signals vanish and are replaced by those of the [1+1] complexes. From these observations, the new signals can be ascribed to the pyrrole NH peaks of the [2+1 (= receptors + anion)] binding complexes (**3a**−**c**)$_2$·Cl^-. The signals of the bridging CH and the *o*-CH in the [2+1] complexes are observed in the intermediate region between free **3a**−**c** and the [1+1] complexes **3a**−**c**·Cl^-, for example, those of the bridging CH and *o*-CH in **3a**$_2$·Cl^- appear at 8.5 and 7.7 ppm, respectively, with 0.6 equiv of TBACl. The 2:1 complexes of aryl-substituted receptors and Cl^- at low temperature were supported by ^{1}H DOSY NMR measurement of the derivative **3c**, wherein the diffusion constant of **3c**$_2$·Cl^- was smaller than that of **3c**. Electrospray ionization time-of-flight mass spectrometry (ESI-TOF-MS) of **3a**−**c** with 0.3 equiv

(19) Choi, K.; Hamilton, A. D. *J. Am. Chem. Soc.* **2003**, *125*, 10241−10249.

(20) The downfield shifts of signals due to protons at the interaction sites (*o*-CH, pyrrole NH, and bridging CH) in the [1+1]-type Cl^- complexes **3a**−**c**·Cl^- are also observed. In the case of **3a** with 1.5 equiv of Cl^-, $\Delta\delta$ values are 0.53 (*o*-CH), 2.53 (pyrrole NH), and 2.41 (bridging CH) ppm, respectively. On the other hand, the corresponding values for **3b** and **3c** with 3 and 5 equiv of Cl^- are 0.36 (*o*-CH), 2.56 (pyrrole NH), and 2.31 (bridging CH) ppm for **3b** and 2.54 (pyrrole NH) and 2.12 (bridging CH) ppm for **3c**, respectively.

of TBACl in CH_3CN (1×10^{-6} M) in a negative mode also suggests the formation of the [1+1] and [2+1] binding complexes (see the Supporting Information).[21] DFT studies at the B3LYP/6-31G** level and semiempirical calculations at the AM1 level[22] both provide possible geometries for [1+1] and [2+1] binding modes with anions (Cl^-), respectively.[23] Multiple binding modes make the system more complicated; however, the association constants for the [1+1] binding complexes in Table 1 can be estimated under dilute and ambient conditions, in order to exclude the possibility of the [2+1] complexes.

^{1}H NMR measurements for the Cl^- complexation of **3a**−**c** from 40 to −90 °C in CD_2Cl_2 suggest significant changes in the ratios of the [1+1] and [2+1] complexes. In the case of phenyl-substituted **3a** with 0.3 equiv of Cl^-, both the anion-free receptor and the [1+1] complex **3a**·Cl^- (labeled by plus marks, Figure 3) are observed in the range from 40 to −30 °C, and at temperatures lower than −40 °C, the resonances ascribable to the [2+1] complex **3a**$_2$·Cl^- (labeled by asterisks) also emerge. Similarly, the [2+1] complexes of **3b** and **3c** are observed at temperatures below −20 and −10 °C, respectively, under the same conditions (see the Supporting Information).

While the binding constants for the [1+1] and [2+1] complexes (K_{a11}, K_{a21}) based on the concentrations of the free receptors and anion are essential for representing of the stability

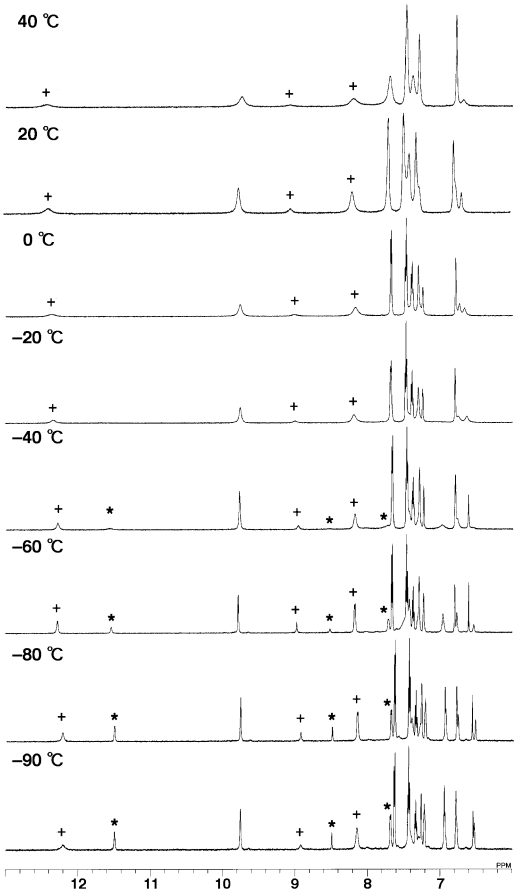

Figure 3. Variable-temperature ^{1}H NMR spectral changes of **3a** (1×10^{-3} M) from 40 to −90 °C in CD_2Cl_2 with 0.3 equiv of Cl^- added as a TBA salt (the signals of [2+1] and [1+1] are labeled by asterisks and plus marks, respectively).

of each complex, the association constants K_a, defined by the equations (e.g., those for **3a**) described below,

$$K_a = K_{a21}/K_{a11} = \frac{[\mathbf{3a}_2\cdot Cl^-]}{[\mathbf{3a}]\,[\mathbf{3a}\cdot Cl^-]}$$

$$K_{a11} = \frac{[\mathbf{3a}\cdot Cl^-]}{[\mathbf{3a}]\,[Cl^-]}$$

$$K_{a21} = \frac{[\mathbf{3a}_2\cdot Cl^-]}{[\mathbf{3a}]^2\,[Cl^-]}$$

are also adequate parameters to indicate the status of [2+1] binding (K_{a21}) relative to that of the [1+1] binding (K_{a11}) derived from the integrals of the ^{1}H NMR peaks at each temperature. Actually, the K_a of **3c**, for example, at −70 °C is 2500 M^{-1}, which is larger than those of **3a** (550 M^{-1}) and **3b** (1500 M^{-1}) (Table 2).[24] The order of K_a, **3a** < **3b** < **3c**, at each temperature is consistent with the qualitative data obtained from the ESI-TOF-MS analysis.

On the other hand, the smaller F^- anion exhibited binding properties slightly different from those of Cl^-. The structure of **3a**·F^- optimized by DFT calculation, with a slight distortion from planarity caused by its small size relative to Cl^-, has simulated bond lengths at 3.14, 2.63, and 2.89 Å between F^- and the *o*-C(H), the pyrrole N(H), and the bridging C(H),

(21) For example, the peaks observed around 437.10 and 839.24, ascribable to **3a** + Cl^- (exact mass: 437.105) and 2 × **3a** + Cl^- (exact mass: 839.241), respectively, fit the ideal distributions. The intensities of the [2+1] complexes ((**3a**−**c**)$_2$·Cl^-) relative to those of [1+1] (**3a**−**c**·Cl^-) are gradually increased in the order of **3a** < **3b** < **3c**, consistent with the ^{1}H NMR observations, while a quantitative discussion is difficult because the MS peak intensities are always affected by the conditions during ionization rather than those in solution (CH_3CN in this case). See also: Sansone, F.; Chierici, E.; Casnati, A.; Ungaro, R. *Org. Biomol. Chem.* **2003**, *1*, 1802−1809.

(22) Frisch, M. J.; et al. *Gaussian 03*, revision C.01; Gaussian, Inc.: Wallingford CT, 2004.

(23) The optimized [1+1] mode **3a**·Cl^- by DFT affords the speculated bond lengths between the anion and the *o*-C(H), pyrrole N(H), and the bridging C(H) of 3.65, 3.34, and 3.44 Å, respectively. On the other hand, **3b**·Cl^- shows 3.63 Å for *o*-C(H)···Cl^- with a *distorted* pentacoordination, where two aryl rings are tilted at 27.6° (6.1° for **3a**·Cl^-) to the core plane. In contrast, **3c**·Cl^- affords a tricoordinated geometry around the anion with the aryl units rather canted at 59.6°. In the case of anion complexes of **3b** and **3c**, steric repulsion between the β-CH and the *o*-CH_3 as well as the fewer number (*two* and *zero*) of *o*-CH compared to **3a** (*four*) may be the main factors for the suppressed K_{a11}. Since the *preorganized* conformations of the anion-free **3a**−**c** with doubly inverted pyrrole rings are similarly less stable in theory at ca. 8.2−8.8 kcal/mol relative to the most stable ones, the anion-binding affinities of these receptors are determined mainly by the stabilities of the complexes **3a**−**c**·Cl^-. Further, AM1 level calculations also support the [2+1] binding mode (**3a**−**c**)$_2$·Cl^-, observed under low temperature conditions with fewer equivalents of the anion, using 10 hydrogen-bonding interactions by two receptors in the cases of **3a**,**b**. For example, in the optimized structures of **3a**$_2$·Cl^-, the theoretical bond lengths between the anion and the *o*-C(H), pyrrole N(H), and the bridging C(H) are 3.74−3.75, 3.13, and 3.22 Å, respectively.

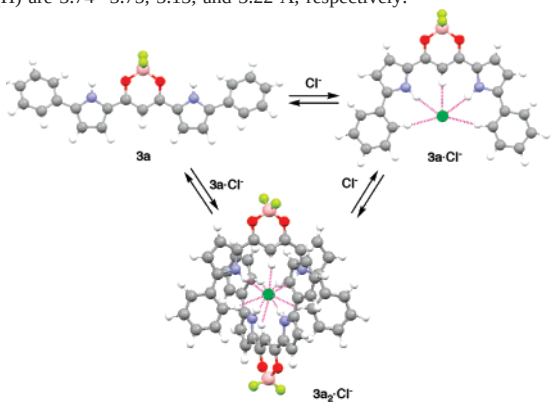

Table 2. Binding Constants K_a (M^{-1}) and Corresponding ΔG^0 (kJ/mol) of Cl^- Binding of **3a**−**c** at Various Temperatures Estimated by ^1H NMR in CD_2Cl_2

	3a		3b		3c	
temp (°C)	K_a	ΔG^0	K_a	ΔG^0	K_a	ΔG^0
−10	−	−	−	−	220	−11.8
−20	−	−	190	−11.0	300	−12.0
−30	−	−	220	−10.9	400	−12.1
−40	270	−10.8	390	−11.6	740	−12.8
−50	320	−10.7	670	−12.1	1300	−13.3
−60	370	−10.5	1000	−12.2	1900	−13.4
−70	550	−10.6	1500	−12.4	2500	−13.2
−80	620	−10.3	1900	−12.1	3400	−13.0
−90	780	−10.1	2300	−11.7	4800	−12.9

respectively. The changes in ^1H NMR spectra of **3a**−**c** during F^--binding in CD_2Cl_2 from 40 to −90 °C afforded the observations that, in the presence of small amounts of F^- as its TBA salt, the signals due to the *o*-CH, the pyrrole NH, and the bridging CH diminish and new ones appear in the downfield region. However, excess quantities of F^- gave complicated resonances of **3a**,**b** presumably containing those due to the deprotonated species. From the above observations for Cl^- and F^-, acyclic anion receptors give various binding modes, depending on receptors and conditions.

Rotations of Pyrrole Rings by Anion Complexation. Artificial molecular motors have been achieved by inter- and intramolecular interactions such as hydrogen bonding and metal coordination of rather rigid π-conjugated components.[25] In the cases of **3a**−**c** as well as **1b**,**c**, the signals ascribable to, especially, the pyrrole NH and the bridging CH of the anion-free **3a**−**c** and the [1+1] coordinated species **3a**−**c**·X^- can be observed independently,[26] which implies that the inversions of the pyrrole rings assisted by anion binding are slow on the NMR time scale. The rate constants *k* for F^--, Cl^--, and Br^--binding of **3a**, as the representative of the receptors, using TBA salts in CH_2Cl_2 at 25 °C have been estimated to be 7.2×10^4, 13.0×10^4, and 6.0×10^4 M^{-1} s^{-1}, respectively, by stopped-flow measurements.[27,28] While the order of *k*, $Cl^- > Br^-$, is consistent with that of the binding constants (K_{a11}), the more associated F^- shows an intermediate value between that of Cl^- and Br^-, suggesting that thermodynamic stability is not always correlated with the kinetic properties.

Apart from the equilibrium processes for anion binding discussed above, the pyrrole rotations of the free receptors **3a**−**c** and those of the complexes **3a**−**c**·X^- are not contemplated here because of the miniscule ratios (∼0) of the "preorganized (inverted)" geometries for the former and the "β-CH-binding" of the latter, respectively, as suggested by the DFT calculations. Also, in contrast to pyrrole inversions, the α-aryl ring rotations of **3a**−**c** are too fast to allow the determination of the kinetic constants of the anion-free forms. Similarly, such rotations of the anion complexes, probably slower than those of the free receptors, are still excessive, as derived from the single NMR signals of the associated *o*-CH, although we have tried to regulate the rotation of aryl rings according to the binding of negatively charged species.

Efficient Colorimetric and Fluorescent Anion Sensors. The fluorescence emission of **3a**−**c** at 529, 525, and 499 nm, excited at their absorption maxima in CH_2Cl_2, is shifted and almost completely quenched by the addition of F^-. The addition of excess F^- affords new fluorescence bands at 558 and 557 nm for **3a**,**b**, respectively, possibly derived from the partial formation of the deprotonated species. A rather weak band at 527 nm is also observed in **3c**. In contrast, other anions had almost no effect on the fluorescence intensity and the emission wavelength (λ_{em}). The above findings suggest that the aryl-substituted BF_2 complexes could be made to function as more efficient and quantitative F^- sensors than the derivatives reported so far. This point is underscored in Figure 4a, which shows the changes in color and fluorescence induced by the addition of F^- and Cl^- to a CH_2Cl_2 solution of **3a**−**c**. According to the substituents, the receptors **3a**−**c** as well as **1a** (λ_{em} = 451 nm) and **1b** (λ_{em} = 474 nm), as references, exhibit remarkably distinct color and fluorescence. As expected from the spectral changes, Cl^- (2−5 equiv) affords hues almost identical to those of the anion-free receptors. While sufficient quantities of F^- (2−5 equiv) resulted in almost complete quenching, large excesses (20 equiv) gave a new orange-colored emission for **3a**,**b**. The molecular orbitals (HOMO and LUMO) of **3a**−**c** estimated at the B3LYP/6-31+G**//B3LYP/6-31G** level suggest the extension of π-conjugation by the aryl moieties (Figure 4b). Therefore, π-conjugation is correlated with the coplanarity of the core unit and the aryl side planes. In fact, the energy gaps between the HOMO and the LUMO (3.084, 3.148, 3.385, 3.578, and 3.431 eV for **3a**−**c** and **1a**,**b**, respectively) are related to the absorption bands as observed in the electronic spectral analyses.

Emissive Supramolecular Organogel Formation Controlled by Anions. Aryl substitution at the α-positions of pyrrole, as seen in the systems **3a**−**c**, enables various substituents to be introduced in these new classes of acyclic anion receptors for further applications. Therefore, derivatives with alkoxy chains of various lengths at the aryl rings (**5a**−**d**) have been synthesized via the corresponding diketones **4a**−**d** by the procedures similar to those for **3a**−**c** (Figure 5a).[29] The X-ray structure of **5a** shows the *two* tetrameric and *one* trimeric stacking structures, exhibiting various slipped assemblies in the solid state (Figure 5b). Hydrogen-bonding interactions between

(24) The van't Hoff plots of **3b** and **3c** suggest the possibility of the conformation changes of the host molecules, [1+1] and/or [2+1] complexes, depending on the temperatures. The thermodynamic parameters for Cl^- bindings of **3a**−**c** estimated by van't Hoff plots below −50 °C, ΔH^0 = −7.8 (**3a**), −10.5 (**3b**), and −10.8 (**3c**) kJ/mol; ΔS^0 = +13.2 (**3a**), +7.9 (**3b**), and +11.5 (**3c**) J/mol·K, and those of **3b** and **3c** above −40 °C, ΔH^0 = −18.0 (**3b**) and −20.1 (**3c**) kJ/mol; ΔS^0 = −28.1 (**3b**) and −32.1 (**3c**) J/mol·K, suggest the enthalpy-driven equilibrium systems due to the relatively small ΔS^0. In contrast to **3b** and **3c** above −40 °C, showing the "ordinary" negative ΔS^0 for binding processes, the positive ΔS^0 values of **3a**−**c** below −50 °C, which may be within the error, are possibly derived from the release from the tightly bound [1+1] complex **3a**−**c**·Cl^-. See also: Smithrud, C. B.; Wyman, T. B.; Diederich, F. *J. Am. Chem. Soc.* **1991**, *113*, 5420−5426.

(25) (a) Oki, M. *The Chemistry of Rotational Isomers*; Springer: Berlin, 1993. (b) Kelly, T. R.; Bowyer, M. C.; Bhaskar, K. V.; Bebbington, D.; Garcia, A.; Lang, F.; Kim, M. H.; Jette, M. P. *J. Am. Chem. Soc.* **1994**, *116*, 3657−3658. (c) Bedart, T.; Moore, J. S. *J. Am. Chem. Soc.* **1995**, *117*, 10662−10671. (d) Balzani, V.; Credi, A.; Raymo, F. M.; Stoddart, J. F. *Angew. Chem., Int. Ed.* **2000**, *39*, 3348−3391. (e) Balzani, V.; Venturi, M.; Credi, A. *Molecular Devices and Machines; A Journey to the Nanoworld*; Wiley-VCH: Wienheim, 2003.

(26) β-Ethyl derivatives have exhibited the coalesced resonances between the anion complexes and receptors in CD_2Cl_2 at rt. See also ref 14f.

(27) (a) Hirose, J.; Inoue, K.; Sakuragi, H.; Kikkawa, M.; Minakami, M.; Morikawa, T.; Iwamoto, H.; Hiromi, K. *Inorg. Chim. Acta* **1998**, *273*, 204−212. (b) Sato, M.; Kanamori, T.; Kamo, N.; Demura, M.; Nitta, K. *Biochemistry* **2002**, *41*, 2452−2458.

(28) Rate constants cannot be determined by ^1H NMR exchange studies due to the equilibrium of the host−guest complexation. See: Kaplan, J. I.; Fraenkel, G. *NMR of Chemically Exchanging Systems*; Academic Press: New York, 1980.

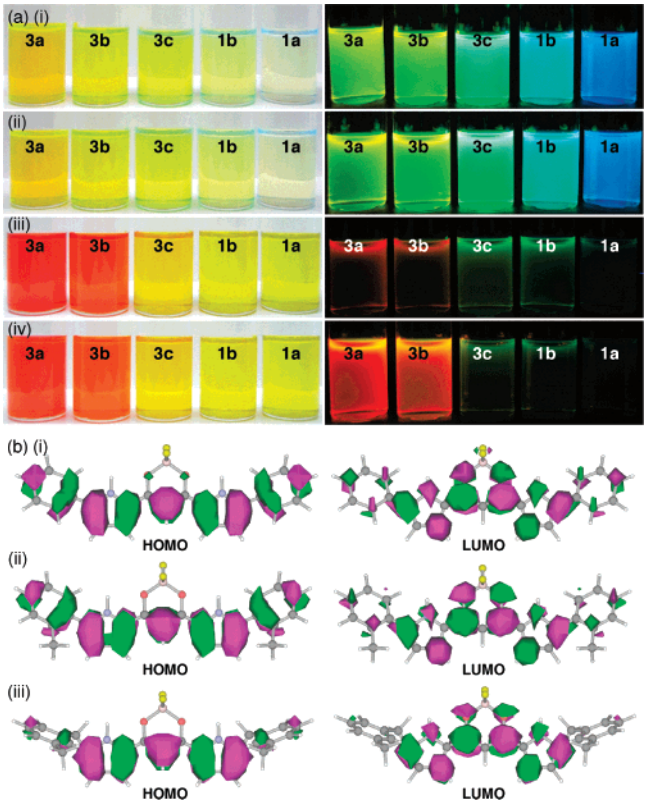

Figure 4. (a) Color (left) and fluorescence emission (right) changes of **3a**−**c**, **1b**, and **1a** in CH_2Cl_2 (5×10^{-4} M) by (i) no anion, (ii) Cl^- (2 equiv for **3a**, 3 equiv for **3b**, and 5 equiv for **3c**, **1b**, and **1a**), (iii) a small amount of F^- (2 equiv for **3a**, 3 equiv for **3b**, and 5 equiv for **3c**, **1b**, and **1a**), and (iv) excess F^- (20 equiv). (b) HOMO and LUMO of (i) **3a**, (ii) **3b**, and (iii) **3c**.

N−H···F−B are also observed, although dimers such as those observed for **3a**,**b** (Figure 1a) are not formed. Furthermore, X-ray analysis of the anion complex **5a**·Cl^-, exhibiting a pentacoordinated geometry similar to that of **3a**·Cl^-, with the distances of 3.265−3.351 Å (N(−H)···Cl), 3.403 and 3.417 Å (C(−H)···Cl), and 3.604−3.688 Å (*o*-C(−H)···Cl), suggests the formation of π-stacking and an electrostatically mediated columnar structure consisting of two **5a**·Cl^- planes and a layer of the two TBA cations (Figure 5c). The distances between the two neighboring Cl^- ions along this column are 5.713 and 8.263 Å.

Long aliphatic chains make the anion receptors soluble in various hydrocarbon solvents at low concentration. For example, the BF_2 complex **5d** shows absorption bands at 521 nm in CH_2Cl_2 and 493 nm in octane (1×10^{-5} M). The modest blue-shift in the nonpolar solvent (octane) under dilute conditions is derived from the solvent effect stabilizing the ground state of neutral molecules and excludes the possibility of aggregation using the core π-plane stacking.

Of the receptors with aliphatic alkoxy chains, the hexadecyloxy-substituted **5d** affords a transparent emissive gel in

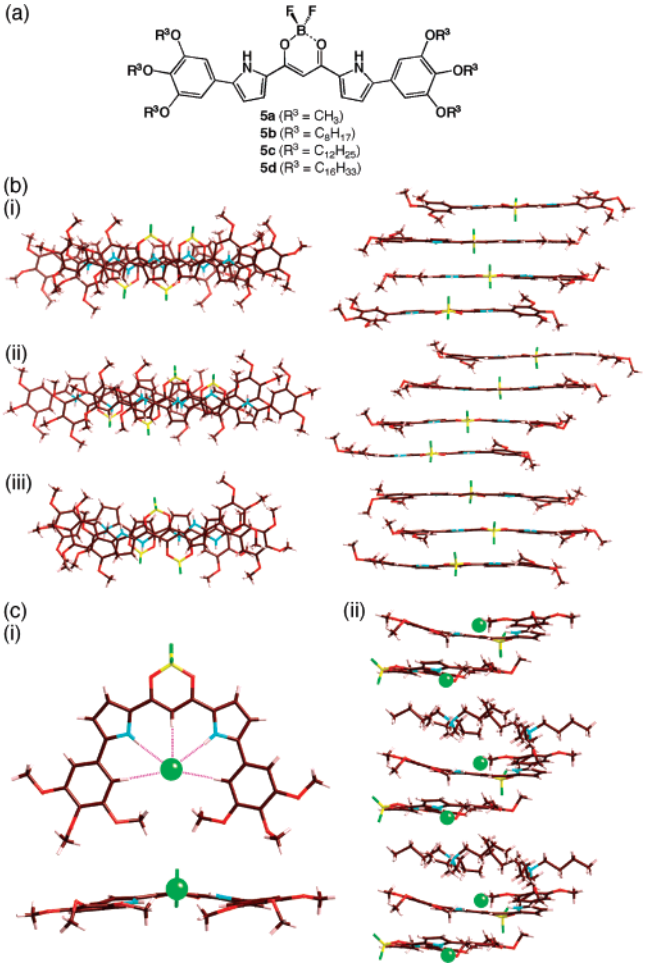

Figure 5. (a) BF_2 complexes **5a**−**d** with 3,4,5-trisubstituted aryl rings. (b) Stacking structures ((i, ii) two kinds of tetramers and (iii) trimer, top and side views) of **5a** in the solid state. (c) (i) Single-crystal X-ray structure (top and side views) of Cl^- complex of **5a** (one of the two conformations) and (ii) columnar structure. Solvents are omitted for clarity.

hydrocarbon solvents such as octane (critical concentration = 10 mg/mL), where the UV/vis absorption bands detected using a quartz spacer are observed at 525 nm with shoulders at ca. 470 and 555 nm. These split bands are possibly derived from the slipped *H*- and *J*-aggregated modes and the incomplete parallel orientation of the molecules.[30] Fluorescence emission from the organogel is detected at 654 nm ($\lambda_{ex} = 470$ nm), which is red-shifted compared to $\lambda_{em} = 533$ nm and $\lambda_{ex} = 493$ nm of a dilute octane solution (1×10^{-5} M). Other solvents such as hexane and decane gave similar gel states, and cyclohexane and methylcyclohexane slowly afforded an opaque organogel after standing for 1 day. Upon heating above 27.5 °C, a sol−gel transition ($T_{sol-gel}$) occurs for the red organogel of **5d** in octane to give a solution that returns to the gel state upon cooling below $T_{sol-gel}$ (Figure 6). The dodecyloxy derivative **5c** (10 mg/mL) exhibits a $T_{sol-gel}$ at 4.5 °C for the octane gel, while the octyloxy-substituted **5b** (10 mg/mL) forms an organogel at −8.5 °C, which is lower than those of **5c**,**d**.

In order to obtain details regarding the organogel **5d**, atomic force microscopy (AFM) was performed. The AFM observations of the octane gel of **5d** at 10 mg/mL, cast by spin-coating on a Si substrate and dried for 1 h in a desiccator, afforded organized

(29) The anion-binding constants K_{a11} of **5a**, determined by UV/vis absorption spectral changes in CH_2Cl_2, are 250,000 (F^-), 360,000 (Cl^-), 19,000 (Br^-), 980,000 ($CH_3CO_2^-$), 210,000 ($H_2PO_4^-$), and 860 (HSO_4^-) M^{-1}, which are larger than those of **3a** except for F^-. The derivatives with long alkyl chains (**5b**−**d**) are less suitable for K_{a11} determination due to the lower solubility as compared with **5a** in CH_2Cl_2. As the preorganized structure of **5a** optimized by DFT calculation is 8.08 kcal/mol less stable than the most stable conformation, like **3a**−**c**, the pendant methoxy moieties may stabilize the binding anion.

(30) Kasha, M.; Rawls, H. R.; El-Bayoumi, M. A. *Pure Appl. Chem.* **1965**, *11*, 371−392.

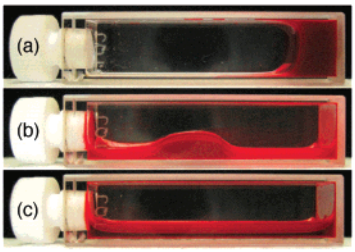

Figure 6. Phase transition of **5d** in octane (10 mg/mL) between sol and gel at (a) 25.0, (b) 27.5, and (c) 30.0 °C.

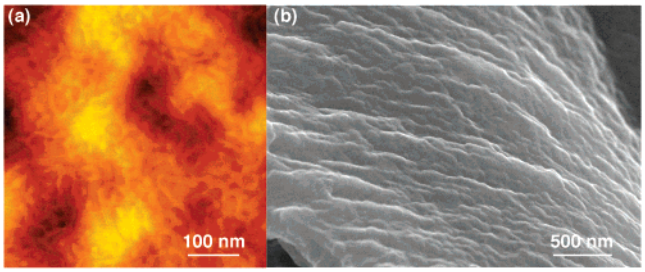

Figure 7. (a) AFM 2D image in a tapping mode of **5d** (from octane gel) cast by spin-coating on a silicon substrate and (b) SEM image of xerogel **5d** from octane at a cracked edge of a gold-coated quartz plate.

rope-like structures with a width of ca. 10 nm, formed from the molecular-level 1D assemblies (Figure 7a). Such strands gather to give larger morphologies at the 100−200-nm scale, which is also observed by scanning electron microscopy (SEM) at a cracked edge of a gold-coated quartz plate to obtain the cross-sectional images (Figure 7b). Supramolecular organogel formation is achieved for these ordered structures on the basis of noncovalent interactions between the π-conjugated moieties and their substituents.

Highly ordered structures were suggested by X-ray diffraction analysis (XRD) of a film fabricated by casting an octane gel of **5d**, drying at 60 °C under vacuum, and aging at 5 °C for 12 h prior to measurement, with peaks at $2\theta = 2.43°$ (001), 4.89° (002), and 7.32° (003). The *d*-value of ca. 3.62 nm (001) presumably corresponds to the distance between the stacking wires of **5d**. Although further details should be investigated, the possible molecular-level stacking structures, also suggested by the X-ray analysis of **3a**,**b** and **5a** as well as molecular modeling of **5d**, can be correlated with the excitonic coupling between the chromophores.[31]

Organized soft materials such as the supramolecular organogels described here can be controlled by an external stimulus. Thus, the addition of Cl^- (10 equiv) as its TBA salt (solid Bu_4NCl) to the octane gel of **5d** at 20 °C effected a gradual decomposition of the gelatinous state in ca. 2 h, yielding an orange-colored and highly emissive solution (Figures 8a,b). The absorption maximum and the corresponding fluorescence emission of the concentrated octane solution (10 mg/mL) including Cl^- were observed at 524 and 574 nm ($\lambda_{ex} = 470$ nm), respectively, suggesting that the receptor **5d** is soluble as the

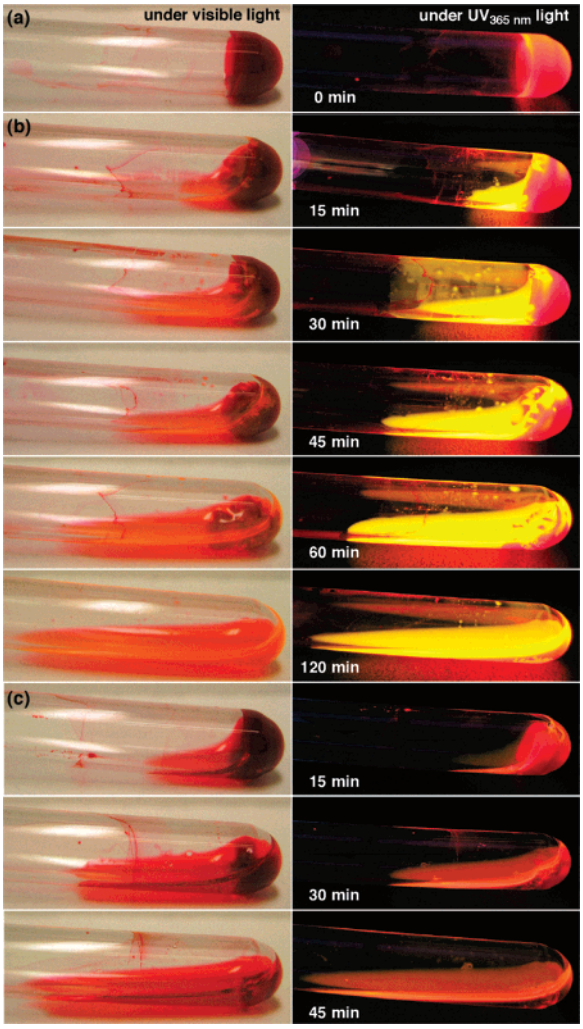

Figure 8. Transition of supramolecular organogel of **5d** in octane (10 mg/mL, (a)) at 20 °C upon the addition of (b) Cl^- (10 equiv) and (c) F^- (10 equiv) added as solid TBA salts.

"monomeric" anion complex in octane solution.[32] Heating the gel with Bu_4NCl > ca. 30 °C promptly resulted in the solution. The addition of Br^- partially transformed the gel to solution in 2−3 days under similar conditions, while $CH_3CO_2^-$ exhibited the transition in ca. 3 h. The slow gel collapse by these anions can be correlated with the pyrrole ring inversion to the π-stacking situation required for anion-binding, and is a unique property of these acyclic receptors.[14] On the other hand, the rapid change to the solution state induced by F^- (10 equiv) as its TBA salt at 20 °C (Figure 8a,c) is ascribable to the peculiar binding behavior of F^- to the NH site(s) without the pyrrole ring inversion(s) if not required.[14b] The F^- complex of **5d** in octane affords a λ_{max} at 504 nm with a shoulder at 527 nm and λ_{em} at 578 and 606 nm ($\lambda_{ex} = 470$ nm). In contrast to the activities of anions such as F^-, Cl^-, and Br^-, the addition of Bu_4NPh_4B induces no transition to the solution phase even after heating, which supports the assumption that the anions, not TBA cations, are responsible for the transformation of the organogel to solution. While the correlation with the rate constants *k* (M^{-1}

(31) The solid-state UV/vis absorption analysis of **5a** has exhibited broad and split bands like those of the gelated **5d** in octane; this supports the relation between the packing structure of **5a** and expected stacking mode of **5d** in the organogel, although the detailed structures of organogel cannot be speculated.

(32) Fluorescence spectra of the octane gel of **5d** with small amounts of Cl^- (0.1, 0.5, and 0.75 equiv) as its tetrabutylammonium salt, which can form a gel state, are exhibited at 648, 606, and 578 nm, respectively, derived from the sum of the emissions of the receptor and the anion complex; this result can exclude the energy transfer process in this assembled system.

s^{-1}) of the anion-binding processes of **3a** in solution is observed in the cases of Cl^- and Br^-, the fast transition to solution by F^- is explained by the specific affinity of this anion for an NH site, as mentioned above. Supramolecular assemblies such as organogels amplify the rigidity of the stable conformations of monomers by means of a $\pi-\pi$ stacking; therefore, the organized structures controlled by the anion identity are in contrast with the behavior of each molecule exhibiting dynamic conformational changes in the solution state.

Summary

Aryl substitution at the α-positions of pyrrole of the acyclic oligopyrrole anion receptors exhibits efficient guest binding using the *o*-CH sites, drastic colorimetric and fluorescent changes in the presence of anions, and more essentially, the effective formation of $\pi-\pi$ stacking structures. In addition, various substituents can be readily attached to the receptor units via aryl moieties for further applications. In fact, the introduction of long aliphatic chains on the aryl rings affords transparent emissive gels, which can be modulated by external chemical stimuli. Further, the modification of the additives, including countercations and solvents as well as anions used, could yield functional materials including supramolecular organogels, liquid crystals, films, etc. On the other hand, hydrophilic aryl moieties at the periphery result in aggregations and potentially efficient sensors in water.[33] Additionally, aryl-bridged oligomeric systems with aliphatic or hydrophilic chains will be prepared in the near future for the observation of anion-stimulated dynamic conformation changes.

Experimental Section

Starting materials were purchased from Wako Chemical Co., Nacalai Chemical Co., and Aldrich Chemical Co. and used without further purification unless otherwise stated. UV−visible spectra were recorded on a Hitachi U-3500 spectrometer for the solution and gel states and a System Instruments surface and interface spectrometer SIS-50 for the solid state. Fluorescence spectra were recorded on a Hitachi F-4500 fluorescence spectrometer for ordinary solution and a Hamamatsu Quantum Yields Measurements System for Organic LED Materials C9920-02 for organogel and its solution. NMR spectra used in the characterization of products were recorded on a JEOL ECA-600HR 600 MHz spectrometer. All NMR spectra were referenced to solvent. Fast atom bombardment mass spectrometric studies (FAB-MS) were made using a JEOL-GCmate instrument in the positive ion mode with a 3-nitrobenzylalcohol matrix. Electrospray ionization mass spectrometric studies (ESI-MS) were recorded on a BRUKER microTOF using negative mode ESI-TOF method. TLC analyses were carried out on aluminum sheets coated with silica gel 60 (Merck 5554). Column chromatography was performed on Sumitomo alumina KCG-1525, Wakogel C-200, C-300, and Merck silica gel 60 and 60H. 2-Phenylpyrrole was synthesized by the literature procedures.[17]

Synthesis of 1-*tert*-Butoxycarbonyl-2-(2-tolyl)pyrrole and 2-(2-Tolyl)pyrrole. To a solution of 2-bromotoluene (342.0 mg, 2.0 mmol), 1-*tert*-butoxycarbonylpyrrole-2-boronic acid (506.5 mg, 2.4 mmol), and tetrakis(triphenylphosphine)palladium(0) (116.0 mg, 0.10 mmol) in 1,2-dimethoxyethane (30 mL) at room temperature under nitrogen was added a solution of Na_2CO_3 (763.1 mg, 7.2 mmol) in water (2 mL). The mixture was heated at reflux for 4 h, cooled, and then partitioned between water and CH_2Cl_2. The combined extracts were dried over anhydrous $MgSO_4$ and evaporated to give an oil. The residue was then chromatographed over flash silica gel column (eluent: CH_2Cl_2/hexane = 1/3) to give 1-*tert*-butoxycarbonyl-2-(2-tolyl)pyrrole (192.6 mg, 37%) as a colorless oil. R_f = 0.24 (CH_2Cl_2/hexane = 1/3). ^{1}H NMR (600 MHz, $CDCl_3$, 20 °C): δ (ppm) 7.37 (m, 1H, pyrrole-H), 7.25−7.23 (m, 4H, Ar-H), 6.24 (m, 1H, pyrrole-H), 6.07 (m, 1H, Ar-H), 2.12 (s, 3H, CH_3), 1.24 (s, 9H, Boc). FABMS: *m*/*z* (% intensity): 257.2 (100, M^+), 258.2 (40, $M^+ + 1$). Calcd for $C_{16}H_{19}NO_2$: 257.14. To the product 1-*tert*-butoxycarbonyl-2-(2-tolyl)pyrrole (125.2 mg, 0.487 mmol) was added ethylene glycol (5 mL) and was heated at reflux (180 °C) for 30 min, cooled, and partitioned between water and dichloromethane. The combined extracts were dried over anhydrous $MgSO_4$ and evaporated to give an oil. The residue was then chromatographed over flash silica gel column (eluent: CH_2Cl_2/hexane = 1/1) to give 2-(2-tolyl)pyrrole as a colorless oil (61.9 mg, 80%). R_f = 0.44 (CH_2Cl_2/hexane = 1/1). ^{1}H NMR (600 MHz, $CDCl_3$, 20 °C): δ (ppm) 8.28 (br, 1H, NH), 7.35 (dd, J = 7.8, 1.2 Hz, 1H, pyrrole-H), 7.25−7.18 (m, 3H, Ar-H), 6.88 (m, 1H, pyrrole-H), 6.35 (m, 1H, pyrrole-H), 6.32 (m, 1H, pyrrole-H), 2.46 (s, 3H, CH_3). FABMS: *m*/*z* (% intensity): 157.1 (100, M^+), 158.1 (38, $M^+ + 1$). Calcd for $C_{11}H_{11}N$: 157.08.

Synthesis of 1-*tert*-Butoxycarbonyl-2-(3-tolyl)pyrrole and 2-(3-Tolyl)pyrrole. To a solution of 3-bromotoluene (342.0 mg, 2.0 mmol), 1-*tert*-butoxycarbonylpyrrole-2-boronic acid (506.5 mg, 2.4 mmol), and tetrakis(triphenylphosphine)palladium(0) (116.0 mg, 0.10 mmol) in 1,2-dimethoxyethane (30 mL) at room temperature under nitrogen was added a solution of Na_2CO_3 (763.1 mg, 7.2 mmol) in water (2 mL). The mixture was heated at reflux for 4 h, cooled, and then partitioned between water and CH_2Cl_2. The combined extracts were dried over anhydrous $MgSO_4$ and evaporated to give an oil. The residue was then chromatographed over flash silica gel column (eluent: CH_2Cl_2/hexane = 1/3) to give 1-*tert*-butoxycarbonyl-2-(3-tolyl)pyrrole (359.9 mg, 70%) as a colorless oil. R_f = 0.31 (CH_2Cl_2/hexane = 1/3). ^{1}H NMR (600 MHz, $CDCl_3$, 20 °C): δ (ppm) 7.33 (m, 1H, pyrrole-H), 7.23 (m, 1H, Ar-H), 7.14−7.10 (m, 3H, Ar-H), 6.22 (m, 1H, pyrrole-H), 6.17 (m, 1H, pyrrole-H), 2.37 (s, 3H, CH_3), 1.34 (s, 9H, Boc). FABMS: *m*/*z* (% intensity): 257.2 (100, M^+), 258.2 (80, $M^+ + 1$). Calcd for $C_{16}H_{19}NO_2$: 257.14. To the product 1-*tert*-butoxycarbonyl-2-(3-tolyl)pyrrole (220.0 mg, 0.855 mmol) was added ethylene glycol (5 mL) and was heated at reflux (180 °C) for 30 min, cooled, and partitioned between water and dichloromethane. The combined extracts were dried over anhydrous $MgSO_4$ and evaporated to give an oil. The residue was then chromatographed over flash silica gel column (eluent: CH_2Cl_2/hexane = 1/1) to give 2-(3-tolyl)pyrrole (93.9 mg, 70%) as a colorless oil. R_f = 0.38 (CH_2Cl_2/hexane = 1/1). ^{1}H NMR (600 MHz, $CDCl_3$, 20 °C): δ (ppm) 8.43 (br, 1H, NH), 7.30−7.24 (m, 3H, Ar-H), 7.02 (d, J = 7.2 Hz, 1H, Ar-H), 6.86 (m, 1H, pyrrole-H), 6.51 (m, 1H, pyrrole-H), 6.29 (m, 1H, pyrrole-H). FABMS: *m*/*z* (% intensity): 157.1 (100, M^+), 158.1 (85, $M^+ + 1$). Calcd for $C_{11}H_{11}N$: 157.09.

Synthesis of 1-*tert*-Butoxycarbonyl-2-(2,6-dimethylphenyl)pyrrole and 2-(2,6-Dimethylphenyl)pyrrole. To a solution of 2-bromo-1,3-dimethylbenzene (370.1 mg, 2.0 mmol), 1-*tert*-butoxycarbonylpyrrole-2-boronic acid (506.5 mg, 2.4 mmol), and tetrakis(triphenylphosphine)-palladium(0) (116.0 mg, 0.10 mmol) in 1,2-dimethoxyethane (30 mL) at room temperature under nitrogen was added a solution of NaOH (288.0 mg, 7.0 mmol) in water (2 mL). The mixture was heated at reflux for 14 h, cooled, and then partitioned between water and CH_2Cl_2. The combined extracts were dried over anhydrous $MgSO_4$ and evaporated to give an oil. The residue was then chromatographed over flash silica gel column (eluent: CH_2Cl_2/hexane = 1/3) to give crude 1-*tert*-butoxycarbonyl-2-(2,6-dimethylphenyl)pyrrole with its trace deprotected compound as a white solid (62.5 mg). R_f = 0.30 (CH_2Cl_2/hexane = 1/3). ^{1}H NMR (600 MHz, $CDCl_3$, 20 °C): δ (ppm) 7.40 (m, 1H, pyrrole-H), 7.13 (m, 1H, Ar-H), 7.04 (m, 2H, Ar-H), 6.28 (m, 1H, pyrrole-H), 6.00 (m, 1H, pyrrole-H), 2.05 (s, 6H, CH_3), 1.19 (s, 9H, Boc). Without further purification, to the crude product, 1-*tert*-butoxycarbonyl-2-(2,6-dimethylphenyl)pyrrole (62.5 mg), was added ethylene glycol (5 mL) and was heated at reflux (180 °C) for 30 min, cooled, and partitioned between water and dichloromethane. The combined

(33) Maeda, H.; Ito, Y.; Haketa, Y. Manuscript in preparation.

extracts were dried over anhydrous $MgSO_4$ and evaporated to give a white solid. The residue was then chromatographed over flash silica gel column (eluent: CH_2Cl_2/hexane = 1/1) to give 2-(2,6-dimethylphenyl)pyrrole as a white powder (50.2 mg, 15% from the starting arylbromide). $R_f = 0.26$ (CH_2Cl_2/hexane = 1/3). ^{1}H NMR (600 MHz, $CDCl_3$, 20 °C): δ (ppm) 7.92 (br, 1H, NH), 7.17 (t, $J = 7.2$ Hz, 1H, Ar-H), 7.10 (d, $J = 7.8$ Hz, 2H, Ar-H), 6.86 (m, 1H, pyrrole-H), 6.32 (m, 1H, pyrrole-H), 6.08 (m, 1H, pyrrole-H). FABMS: *m*/*z* (% intensity): 171.1 (100, M^+), 172.1 (100, $M^+ + 1$). Calcd for $C_{12}H_{13}N$: 171.10.

1,3-Di-(5-phenylpyrrol-2-yl)-1,3-propanedione, 2a. Analogous to a literature procedure, a CH_2Cl_2 solution (30 mL) of 2-phenylpyrrole[17] (274.0 mg, 1.92 mmol) was treated with malonyl chloride (161.8 mg, 1.15 mmol) at room temperature and stirred for 3 h at the same temperature. After the consumption of the starting pyrrole was confirmed by TLC analysis, the mixture was washed with saturated, aq Na_2CO_3 and water, dried over anhydrous $MgSO_4$, filtered, and evaporated to dryness. The residue was then chromatographed over flash silica gel column (eluent: 2% MeOH/CH_2Cl_2) and recrystallized from CH_2Cl_2/hexane to afford **2a** (153.9 mg, 45%) as a pale-yellow solid. $R_f = 0.35$ (2% MeOH/CH_2Cl_2). ^{1}H NMR (600 MHz, $CDCl_3$, 20 °C; diketone **2a** is obtained as a mixture of keto and enol tautomers in the ratio of 1:0.28): δ (ppm) keto form 9.56 (br, 2H, NH), 7.58 (m, 4H, Ar-H), 7.43 (m, 4H, Ar-H), 7.33 (m, 2H, Ar-H), 7.16 (m, 2H, pyrrole-H), 6.60 (m, 2H, pyrrole-H), 4.26 (s, 2H, CH); enol form 16.69 (br, 1H, OH), 9.44 (br, 2H, NH), 7.58 (m, 4H, Ar-H), 7.43 (m, 4H, Ar-H), 7.33 (m, 2H, Ar-H), 6.97 (m, 2H, pyrrole-H), 6.64 (m, 2H, pyrrole-H), 6.37 (s, 1H, CH). FABMS: *m*/*z* (% intensity): 354.2 (58, M^+), 355.21 (100, $M^+ + 1$) Calcd for $C_{23}H_{18}N_2O_2$: 354.14.

1,3-Di-(5-(2-tolyl)pyrrol-2-yl)-1,3-propanedione, 2b. A CH_2Cl_2 solution (10 mL) of 2-(2-tolyl)pyrrole (41.8 mg, 0.27 mmol) was treated with malonyl chloride (22.5 mg, 0.16 mmol) at room temperature and stirred for 3 h at the same temperature. After the consumption of the starting pyrrole was confirmed by TLC analysis, the mixture was washed with saturated, aq Na_2CO_3 and water, dried over anhydrous Na_2SO_4, filtered, and evaporated to dryness. The residue was then chromatographed over flash silica gel column (eluent: 3% MeOH/CH_2Cl_2) and recrystallized from CH_2Cl_2/hexane to afford **2b** (23.8 mg, 46%) as a pale-yellow solid. $R_f = 0.35$ (3% MeOH/CH_2Cl_2). ^{1}H NMR (600 MHz, $CDCl_3$, 20 °C; diketone **2b** is obtained as a mixture of keto and enol tautomers in the ratio of 1:0.19): δ (ppm) keto form 9.35 (br, 2H, NH), 7.39 (m, 2H, Ar-H), 7.28−7.27 (m, 6H, Ar-H), 7.18 (m, 2H, pyrrole-H), 6.43 (m, 2H, pyrrole-H), 4.26 (s, 2H, CH), 2.46 (s, 6H, CH_3); enol form 16.65 (br, 1H, OH), 9.26 (br, 2H, NH), 7.43(m, 2H, Ar-H), 7.28−7.27 (m, 6H, Ar-H), 6.98 (m, 2H, pyrrole-H), 6.46 (m, 2H, pyrrole-H), 6.38 (s, 1H, CH), 2.49 (s, 6H, CH_3). FABMS: *m*/*z* (% intensity): 382.1 (73, M^+), 383.2 (100, $M^+ + 1$). Calcd for $C_{25}H_{22}N_2O_2$: 382.17.

1,3-Di-(5-(3-tolyl)pyrrol-2-yl)-1,3-propanedione, 2b′. A CH_2Cl_2 solution (20 mL) of 2-(3-tolyl)pyrrole (81.7 mg, 0.52 mmol) was treated with malonyl chloride (43.6 mg, 0.31 mmol) at room temperature and stirred for 3 h at the same temperature. After the consumption of the starting pyrrole was confirmed by TLC analysis, the mixture was washed with saturated, aq Na_2CO_3 and water, dried over anhydrous Na_2SO_4, filtered, and evaporated to dryness. The residue was then chromatographed over flash silica gel column (eluent: 3% MeOH/CH_2Cl_2) and recrystallized from CH_2Cl_2/hexane to afford **2b′** (35.5 mg, 36%) as a pale-yellow solid. $R_f = 0.35$ (3% MeOH/CH_2Cl_2). ^{1}H NMR (600 MHz, $CDCl_3$, 20 °C; diketone **2b′** is obtained as a mixture of keto and enol tautomers in the ratio of 1:0.21): δ (ppm) keto form 9.53 (br, 2H, NH), 7.38 (m, 4H, Ar-H), 7.31 (m, 2H, Ar-H), 7.16 (m, 2H, pyrrole-H), 7.13 (m, 2H, Ar-H), 6.58 (m, 2H, pyrrole-H), 4.25 (s, 2H, CH), 2.39 (s, 6H, CH_3); enol form 16.71 (br, 1H, OH), 9.42 (br, 2H, NH), 7.38 (m, 4H, Ar-H), 7.31 (m, 2H, Ar-H), 7.13 (m, 2H, Ar-H), 6.96 (m, 2H, pyrrole-H), 6.62 (m, 2H, pyrrole-H), 6.36 (s, 1H, CH), 2.41 (s, 6H, CH_3). FABMS: *m*/*z* (% intensity): 382.2 (72, M^+), 383.2 (100, $M^+ + 1$). Calcd for $C_{25}H_{22}N_2O_2$: 382.17.

1,3-Bis(5-(2,6-dimethylphenyl)pyrrol-2-yl)-1,3-propanedione, 2c. A CH_2Cl_2 solution (10 mL) of 2-(2,6-dimethylphenyl)pyrrole (47.0 mg, 0.27 mmol) was treated with malonyl chloride (23.1 mg, 0.16 mmol) at room temperature and stirred for 3 h at the same temperature. After the consumption of the starting pyrrole was confirmed by TLC analysis, the mixture was washed with saturated, aq Na_2CO_3 and water, dried over anhydrous $MgSO_4$, filtered, and evaporated to dryness. The residue was then chromatographed over flash silica gel column (eluent: 2% MeOH/CH_2Cl_2) and recrystallized from CH_2Cl_2/hexane to afford **2c** (38.7 mg, 69%) as a pale-yellow solid. $R_f = 0.43$ (2% MeOH/CH_2Cl_2). ^{1}H NMR (600 MHz, $CDCl_3$, 20 °C; diketone **2c** is obtained as a mixture of keto and enol tautomers in the ratio of 1:0.18): δ (ppm) keto form 9.11 (br, 2H, NH), 7.21 (m, 2H, Ar-H), 7.19 (m, 2H, pyrrole-H), 7.12−7.09 (m, 4H, Ar-H), 6.20 (m, 2H, pyrrole-H), 4.26 (s, 2H, CH), 2.14 (s, 12H, CH_3); enol form 16.58 (br, 1H, OH), 9.01 (br, 2H, NH), 7.21 (m, 2H, Ar-H), 7.12−7.09 (s, 4H, Ar-H), 6.99 (m, 2H, pyrrole-H), 6.36 (s, 1H, CH), 6.20 (m, 2H, pyrrole H), 2.18 (s, 12H, CH_3). FABMS: *m*/*z* (% intensity): 410.3 (76, M^+), 411.3 (100, $M^+ + 1$). Calcd for $C_{27}H_{26}N_2O_2$: 410.20.

BF_2 Complex of 2a, 3a. To a CH_2Cl_2 solution (230 mL) of diketone **2a** (50.0 mg, 0.14 mmol) was added BF_3·OEt_2 (600.4 mg, 4.23 mmol) and was stirred for 10 min at room temperature. After removal of the solvent, flash silica gel column chromatography (eluent: 2% MeOH/CH_2Cl_2) and crystallization from CH_2Cl_2/hexane afforded **3a** (54.4 mg, 96%) as a red solid. $R_f = 0.35$ (CH_2Cl_2). ^{1}H NMR (600 MHz, $CDCl_3$, 20 °C): δ (ppm) 9.67 (br, 2H, NH), 7.65 (d, $J = 7.2$ Hz, 4H, Ar-H), 7.48 (t, $J = 7.8$ Hz, 4H, Ar-H), 7.39 (t, $J = 7.2$ Hz, 2H, Ar-H), 7.22 (dd, $J = 2.4$, 1.8 Hz, pyrrole-H), 6.74 (dd, $J = 2.4$, 1.8 Hz, 2H, pyrrole-H), 6.55 (s, 1H, CH). UV/vis (CH_2Cl_2, λ_{max} [nm] (ϵ, 10^5 M^{-1} cm^{-1})): 500.0 (1.24). FABMS: *m*/*z* (% intensity): 402.3 (100, M^+), 403.3 (52, $M^+ + 1$). Calcd for $C_{23}H_{17}BF_2N_2O_2$: 402.14. This compound was further characterized by X-ray diffraction analysis.

BF_2 Complex of 2b, 3b. To a CH_2Cl_2 solution (60 mL) of diketone **2b** (23.0 mg, 0.06 mmol), was added BF_3·OEt_2 (255.5 mg, 1.8 mmol) and was stirred for 10 min at room temperature. After removal of the solvent, flash silica gel column chromatography (eluent: CH_2Cl_2) and crystallization from CH_2Cl_2/hexane afforded **3b** (21.7 mg, 84%) as a vermillion red solid. $R_f = 0.40$ (CH_2Cl_2). ^{1}H NMR (600 MHz, $CDCl_3$, 20 °C): δ (ppm) 9.47 (br, 2H, NH), 7.44 (m, 2H, Ar-H), 7.31−7.30 (m, 6H, Ar-H), 7.26−7.24 (m, 2H, pyrrole-H), 6.56 (m, 2H, pyrrole-H), 6.56 (s, 1H, CH), 2.49 (s, 6H, CH_3). UV/vis (CH_2Cl_2, λ_{max} [nm] (ϵ, 10^5 M^{-1} cm^{-1})): 480.0 (0.93). FABMS: *m*/*z* (% intensity): 430.3 (100, M^+), 431.3 (42, $M^+ + 1$). Calcd for $C_{25}H_{21}BF_2N_2O_2$: 430.17. This compound was further characterized by X-ray diffraction analysis.

BF_2 Complex of 2b′, 3b′. To a CH_2Cl_2 solution (30 mL) of diketone **2b′** (15.0 mg, 0.039 mmol) was added BF_3·OEt_2 (167.5 mg, 1.2 mmol) and was stirred for 10 min at room temperature. After removal of the solvent, flash silica gel column chromatography (eluent: 1% MeOH/CH_2Cl_2) and crystallization from CH_2Cl_2/hexane afforded **3b′** (14.7 mg, 87%) as a red solid. $R_f = 0.36$ (CH_2Cl_2). ^{1}H NMR (600 MHz, $CDCl_3$, 20 °C): δ (ppm) 9.63 (br, 2H, NH), 7.44 (m, 4H, Ar-H), 7.35 (t, $J = 7.8$ Hz, 2H, Ar-H), 7.21 (m, 2H, Ar-H), 7.19 (m, 2H, pyrrole-H), 6.72 (m, 2H, pyrrole-H), 6.54 (s, 1H, CH), 2.44 (s, 6H, CH_3). UV/vis (CH_2Cl_2, λ_{max} [nm] (ϵ, 10^5 M^{-1} cm^{-1})): 502.0 (0.83). FABMS: *m*/*z* (% intensity): 430.2 (100, M^+), 431.2 (42, $M^+ + 1$). Calcd for $C_{25}H_{21}BF_2N_2O_2$: 430.17. This compound was further characterized by X-ray diffraction analysis.

BF_2 Complex of 2c, 3c. To a CH_2Cl_2 solution (60 mL) of diketone **2c** (25.0 mg, 0.061 mmol) was added BF_3·OEt_2 (259.7 mg, 1.83 mmol) and was stirred for 10 min at room temperature. After removal of the solvent, flash silica gel column chromatography and crystallization from CH_2Cl_2/hexane afforded **3c** (20.8 mg, 78%) as a yellow solid. $R_f = 0.40$ (CH_2Cl_2). ^{1}H NMR (600 MHz, $CDCl_3$, 20 °C): δ (ppm) 9.24 (br, 2H, NH), 7.27 (m, 2H, pyrrole-H), 7.24 (t, $J = 7.8$ Hz, 2H, Ar-H), 7.12 (d, $J = 7.8$ Hz, 4H, Ar-H), 6.61 (s, 1H, CH), 6.34 (m, 2H, pyrrole-H), 2.17 (s, 12H, CH_3). UV/vis (CH_2Cl_2, λ_{max} [nm] (ϵ, 10^5 M^{-1} cm^{-1})):

456.0 (1.19). FABMS: *m*/*z* (% intensity): 458.3 (100, M^+), 459.3 (45, $M^+ + 1$). Calcd for $C_{25}H_{21}BF_2N_2O_2$: 458.20.

Synthesis of 5-Bromo-1,2,3-trioctyloxybenzene.[34] A mixture of K_2CO_3 (1.41 g, 10.2 mmol) and 5-bromo-1,2,3-trihydroxybenzene (300.0 mg, 1.46 mmol), synthesized by the modified literature methods,[35] and 1-bromooctane (951.0 mg, 4.92 mmol), in dry DMF (100 mL) was stirred at reflux for 24 h. After cooling, the solvent was evaporated. The crude product was taken up in CH_2Cl_2 and washed with water, dried over $MgSO_4$, and evaporated to dryness. The residue was then chromatographed over silica gel column (eluent: CH_2Cl_2/hexane = 1/4) to give 5-bromo-1,2,3-trioctyloxybenzene (462.0 mg, 58%) as a colorless oil. $R_f = 0.33$ (CH_2Cl_2/hexane = 1/3). ^{1}H NMR (600 MHz, $CDCl_3$, 20 °C): δ (ppm) 6.67 (s, 2H, Ar-H), 3.94−3.89 (m, 6H, OCH_2), 1.78 (tt, $J = 7.2$, 6.6 Hz, 4H, OCH_2CH_2), 1.72 (tt, $J = 7.2$, 6.6 Hz, 2H, OCH_2CH_2), 1.47−1.42 (m, 6H, $OC_2H_4CH_2$), 1.36−1.27 (m, 24H, $OC_3H_6C_4H_8CH_3$), 0.89−0.87 (m, 9H, $OC_7H_{14}CH_3$). FABMS: *m*/*z* (% intensity) 540.3 (100, M^+), 541.3 (82, $M^+ + 1$). Calcd for $C_{18}H_{23}NO_5$: 540.32.

Synthesis of 5-Bromo-1,2,3-tridodecyloxybenzene. A mixture of K_2CO_3 (1.41 g, 10.2 mmol), 5-bromo-1,2,3-trihydroxybenzene (300.0 mg, 1.46 mmol), and 1-bromododecane (1.23 g, 4.94 mmol) in dry DMF (100 mL), was stirred at reflux for 24 h. After cooling, the solvent was evaporated. The crude product was taken up in CH_2Cl_2 and washed with water, dried over $MgSO_4$, and evaporated to dryness. The residue was then chromatographed over silica gel column (eluent: CH_2Cl_2/hexane = 1/3) to give 5-bromo-1,2,3-tridodecyloxybenzene (763.0 mg, 74%) as a white solid. $R_f = 0.29$ (CH_2Cl_2/hexane = 1/3). ^{1}H NMR (600 MHz, $CDCl_3$, 20 °C): δ (ppm) 6.66 (s, 2H, Ar-H), 3.93−3.89 (m, 6H, OCH_2), 1.78 (tt, $J = 7.2$, 6.6 Hz, 4H, OCH_2CH_2), 1.71 (tt, $J = 7.2$, 6.6 Hz, 2H, OCH_2CH_2), 1.47−1.42 (m, 6H, $OC_2H_4CH_2$), 1.34−1.26 (m, 48H, $OC_3H_6C_8H_{16}CH_3$), 0.89−0.87 (m, 9H, $OC_{11}H_{22}CH_3$). FABMS: *m*/*z* (% intensity) 708.5 (100, M^+), 709.5 (74, $M^+ + 1$). Calcd for $C_{18}H_{23}NO_5$: 708.51.

Synthesis of 5-Bromo-1,2,3-trihexadecyloxybenzene. A mixture of K_2CO_3 (2.90 g, 21.0 mmol), 5-bromo-1,2,3-trihydroxybenzene (615.0 mg, 3.0 mmol), and 1-bromohexadecane (3.09 g, 10.1 mmol), in dry DMF (150 mL), was stirred at reflux for 24 h. After cooling, the solvent was evaporated. The crude product was taken up in CH_2Cl_2 and washed with water, dried over $MgSO_4$, and evaporated to dryness. The residue was then chromatographed over silica gel column (eluent: CH_2Cl_2/hexane = 1/3) to give 5-bromo-1,2,3-trihexadecyloxybenzene (2.0 g, 76%) as a white solid. $R_f = 0.44$ (CH_2Cl_2/hexane = 1/3). ^{1}H NMR (600 MHz, $CDCl_3$, 20 °C): δ (ppm) 6.67 (s, 2H, Ar-H), 3.95−3.87 (m, 6H, OCH_2), 1.78 (tt, $J = 7.2$, 6.6 Hz, 4H, OCH_2CH_2), 1.71 (tt, $J = 7.2$, 6.6 Hz, 2H, OCH_2CH_2), 1.45−1.42 (m, 6H, $OC_2H_4CH_2$), 1.29−1.23 (m, 72H, $OC_3H_6C_{12}H_{24}CH_3$), 0.89−0.87 (m, 9H, $OC_{15}H_{30}CH_3$). FABMS: *m*/*z* (% intensity) 876.7 (100, M^+), 877.7 (80, $M^+ + 1$). Calcd for $C_{18}H_{23}NO_5$: 876.69.

Synthesis of 1-*tert*-Butoxycarbonyl-2-(3,4,5-trimethoxyphenyl)-pyrrole and 2-(3,4,5-Trimethoxyphenyl)pyrrole. To a solution of 5-bromo-1,2,3-trimethoxybenzene (247.1 mg, 1.0 mmol), 1-*tert*-butoxycarbonylpyrrole-2-boronic acid (253.2 mg, 1.2 mmol), and tetrakis-(triphenylphosphine)palladium(0) (57.8 mg, 0.05 mmol) in 1,2-dimethoxyethane (20 mL) at room temperature under nitrogen was added a solution of Na_2CO_3 (381.6 mg, 3.6 mmol) in water (1 mL). The mixture was heated at reflux for 4 h, cooled, and then partitioned between water and CH_2Cl_2. The combined extracts were dried over anhydrous $MgSO_4$ and evaporated to give an oil. The residue was then chromatographed over flash silica gel column (eluent: 15% EtOAc/hexane) to give 1-*tert*-butoxycarbonyl-2-(3,4,5-trimethoxyphenyl)-pyrrole (316.7 mg, 95%) as a colorless oil. $R_f = 0.36$ (15% EtOAc/hexane). ^{1}H NMR (600 MHz, $CDCl_3$, 20 °C): δ (ppm) 7.34−7.33 (m, 1H, pyrrole-H), 6.57 (s, 2H, Ar-H), 6.23−6.22 (m, 1H, pyrrole-H), 6.20−6.19 (m, 1H, pyrrole-H), 3.87 (s, 3H, OCH_3), 3.85 (s, 6H, OCH_3), 1.38 (s, 9H, Boc). FABMS: *m*/*z* (% intensity) 333.1 (100, M^+), 334.2 (61, $M^+ + 1$). Calcd for $C_{18}H_{23}NO_5$: 333.16. The product 1-*tert*-butoxycarbonyl-2-(3,4,5-trimethoxyphenyl)pyrrole (248.2 mg, 0.744 mmol) was heated at 190 °C for 15 min. The residue was then chromatographed over flash silica gel column (eluent: 40% EtOAc/hexane) and gave 2-(3,4,5-trimethoxyphenyl)pyrrole as a white solid (153.9 mg, 93%). $R_f = 0.33$ (eluent: 40% EtOAc/hexane). ^{1}H NMR (600 MHz, $CDCl_3$, 20 °C): δ (ppm) 8.39 (br, 1H, NH), 6.87−6.86 (m, 1H, pyrrole-H) 6.68 (s, 2H, Ar-H), 6.45−6.44 (m, 1H, pyrrole-H), 6.31−6.29 (m, 1H, pyrrole-H), 3.91 (s, 6H, OCH_3), 3.86 (s, 3H, OCH_3). FABMS: *m*/*z* (% intensity): 233.1 (100, M^+), 234.2 (65, $M^+ + 1$). Calcd for $C_{13}H_{15}NO_3$: 233.11.

Synthesis of 1-*tert*-Butoxycarbonyl-2-(3,4,5-trioctyloxyphenyl)-pyrrole and 2-(3,4,5-Trioctyloxyphenyl)pyrrole. To a solution of 5-bromo-1,2,3-trioctyloxybenzene (443.8 mg, 0.819 mmol), 1-*tert*-butoxycarbonylpyrrole-2-boronic acid (207.4 mg, 0.983 mmol), and tetrakis(triphenylphosphine)palladium(0) (47.3 mg, 0.041 mmol) in 1,2-dimethoxyethane (20 mL) at room temperature under nitrogen was added a solution of Na_2CO_3 (260.0 mg, 2.46 mmol) in water (1 mL). The mixture was heated at reflux for 4 h, cooled, and then partitioned between water and CH_2Cl_2. The combined extracts were dried over anhydrous $MgSO_4$ and evaporated to give an oil. The residue was then chromatographed over flash silica gel column (eluent: 5% EtOAc/hexane) to give 1-*tert*-butoxycarbonyl-2-(3,4,5-trioctyloxyphenyl)-pyrrole (379.7 mg, 74%) as a colorless oil. $R_f = 0.38$ (eluent: 5% EtOAc/hexane). ^{1}H NMR (600 MHz, $CDCl_3$, 20 °C): δ (ppm) 7.33−7.32 (m, 1H, pyrrole-H), 6.51 (s, 2H, Ar-H), 6.21−6.20 (m, 1H, pyrrole-H), 6.17−6.16 (m, 1H, pyrrole-H), 3.96 (m, 6H, OCH_2), 1.81−1.73 (m, 6H, OCH_2CH_2), 1.50−1.42 (m, 6H, $OC_2H_4CH_2$), 1.34 (s, 9H, Boc), 1.33−1.22 (m, 24H, $OC_3H_6C_4H_8CH_3$), 0.89−0.87 (m, 9H, $OC_7H_{14}CH_3$). FABMS: *m*/*z* (% intensity) 627.5 (100, M^+), 628.6 (45, $M^+ + 1$). Calcd for $C_{39}H_{65}NO_5$: 672.49. The product 1-*tert*-butoxycarbonyl-2-(3,4,5-trioctyloxyphenyl)pyrrole (310.3 mg, 0.494 mmol) was heated at 190 °C for 15 min. The residue was then chromatographed over flash silica gel column (eluent: 5% EtOAc/hexane) and gave 2-(3,4,5-trioctyloxyphenyl)pyrrole as a white solid (248.6 mg, 95%). $R_f = 0.18$ (eluent: 5% EtOAc/hexane). ^{1}H NMR (600 MHz, $CDCl_3$, 20 °C): δ (ppm) 8.34 (br, 1H, NH), 6.84−6.83 (m, 1H, pyrrole-H) 6.64 (s, 2H, Ar-H), 6.41−6.40 (m, 1H, pyrrole-H), 6.28−6.27 (m, 1H, pyrrole-H), 4.00 (t, $J = 6.6$ Hz, 4H, OCH_2), 3.95 (t, $J = 6.6$ Hz, 2H, OCH_2), 1.81 (tt, $J = 7.2$, 6.0 Hz, 4H, OCH_2CH_2), 1.75 (tt, $J = 7.2$, 6.6 Hz, 2H, OCH_2CH_2), 1.49−1.45 (m, 6H, $OC_2H_4CH_2$), 1.37−1.24 (m, 24H, $OC_3H_6C_4H_8CH_3$), 0.89−0.87 (m, 9H, $OC_7H_{14}CH_3$). FABMS: *m*/*z* (% intensity): 527.5 (100, M^+), 528.5 (97, $M^+ + 1$). Calcd for $C_{34}H_{57}NO_3$: 527.43.

Synthesis of 1-*tert*-Butoxycarbonyl-2-(3,4,5-tridodecyloxyphenyl)-pyrrole and 2-(3,4,5-Tridodecyloxyphenyl)pyrrole. To a solution of 5-bromo-1,2,3-tridodecyloxybenzene (426.0 mg, 0.60 mmol), 1-*tert*-butoxycarbonylpyrrole-2-boronic acid (151.9 mg, 0.72 mmol), and tetrakis(triphenylphosphine)palladium(0) (40.8 mg, 0.035 mmol) in 1,2-dimethoxyethane (18 mL) at room temperature under nitrogen was added a solution of Na_2CO_3 (228.9 mg, 2.16 mmol) in water (0.8 mL). The mixture was heated at reflux for 4 h, cooled, and then partitioned between water and CH_2Cl_2. The combined extracts were dried over anhydrous $MgSO_4$, and evaporated to give an oil. The residue was then chromatographed over flash silica gel column (eluent: 3% EtOAc/hexane) gave 1-*tert*-butoxycarbonyl-2-(3,4,5-tridodecyloxyphenyl)pyrrole (367.9 mg, 77%) as a white solid. $R_f = 0.22$ (3% EtOAc/hexane). ^{1}H NMR (600 MHz, $CDCl_3$, 20 °C): δ (ppm) 7.33−7.32 (m, 1H, pyrrole-H), 6.51 (s, 2H, Ar-H), 6.21−6.20 (m, 1H, pyrrole-H), 6.16−6.15 (m, 1H, pyrrole-H), 3.96−3.93 (m, 6H, OCH_2), 1.81−1.73 (m, 6H, OCH_2CH_2), 1.49−1.42 (m, 6H, $OC_2H_4CH_2$), 1.34 (s, 9H, Boc), 1.30−1.25 (m, 48H, $OC_3H_6C_8H_{16}CH_3$), 0.89−0.86 (m, 9H, $OC_{11}H_{22}CH_3$). FABMS: *m*/*z* (% intensity) 795.7 (100, M^+), 796.8 (60, $M^+ + 1$). Calcd

(34) Dol, G. C.; Kamer, P. C. J.; van Leeuwen, P. W. N. M. *Eur. J. Org. Chem.* **1998**, 359−364.
(35) Lincker, F.; Bourgun, P.; Masson, P.; Didier, P.; Guidoni, L.; Bigot, J.-Y.; Nicoud, J.-F.; Donnio, B.; Guillon, D. *Org. Lett.* **2005**, *7*, 1505−1508.

for $C_{51}H_{89}NO_5$: 795.67. The product 1-*tert*-butoxycarbonyl-2-(3,4,5-tridodecyloxyphenyl)pyrrole (287.6 mg, 0.361 mmol) was heated at 190 °C for 15 min. The residue was then chromatographed over flash silica gel column (eluent: 5% EtOAc/hexane) to give 2-(3,4,5-tridodecyloxyphenyl)pyrrole as a white solid (239.7 mg, 95%). R_f = 0.28 (5% EtOAc/hexane). ^{1}H NMR (600 MHz, $CDCl_3$, 20 °C): δ (ppm) 8.34 (br, 1H, NH), 6.84−6.83 (m, 1H, pyrrole-H) 6.64 (s, 2H, Ar-H), 6.41−6.40 (m, 1H, pyrrole-H), 6.28−6.27 (m, 1H, pyrrole-H), 4.00 (t, J = 6.6 Hz, 4H, OCH_2), 3.96−3.94 (t, J = 6.6 Hz, 2H, OCH_2), 1.80 (tt, J = 7.2, 6.6 Hz, 4H, OCH_2CH_2), 1.75 (tt, J = 7.2, 6.6 Hz, 2H, OCH_2CH_2), 1.49−1.45 (m, 6H, $OC_2H_4CH_2$), 1.35−1.26 (m, 48H, $OC_3H_6C_8H_{16}CH_3$), 0.89−0.87 (m, 9H, $OC_{11}H_{22}CH_3$). FABMS: *m*/*z* (% intensity): 695.6 (77, M^+), 696.6 (100, $M^+ + 1$). Calcd for $C_{46}H_{81}NO_3$: 695.62.

Synthesis of 1-*tert*-Butoxycarbonyl-2-(3,4,5-trihexadecyloxyphenyl)pyrrole and 2-(3,4,5-Trihexadecyloxyphenyl)pyrrole. To a solution of 5-bromo-1,2,3-trihexadecyloxybenzene (878.3 mg, 1.0 mmol), 1-*tert*-butoxycarbonylpyrrole-2-boronic acid (253.2 mg, 1.2 mmol), and tetrakis(triphenylphosphine)palladium(0) (57.8 mg, 0.050 mmol) in 1,2-dimethoxyethane (20 mL) at room temperature under nitrogen was added a solution of Na_2CO_3 (381.6 mg, 3.0 mmol) in water (1 mL). The mixture was heated at reflux for 4 h, cooled, and then partitioned between water and CH_2Cl_2. The combined extracts were dried over anhydrous $MgSO_4$ and evaporated to give a solid. The residue was then chromatographed over flash silica gel column (eluent: 3% EtOAc/hexane) to give 1-*tert*-butoxycarbonyl-2-(3,4,5-trihexadecyloxyphenyl)-pyrrole (775.5 mg, 88%) as a white solid. R_f = 0.37(eluent: 5% EtOAc/hexane). ^{1}H NMR (600 MHz, $CDCl_3$, 20 °C): δ (ppm) 7.33−7.32 (m, 1H, pyrrole-H), 6.51 (s, 2H, Ar-H), 6.21−6.19 (m, 1H, pyrrole-H), 6.16−6.15 (m, 1H, pyrrole-H), 3.96−3.93 (m, 6H, OCH_2), 1.81−1.73 (m, 6H, OCH_2CH_2), 1.49−1.42 (m, 6H, $OC_2H_4CH_2$), 1.34 (s, 9H, Boc), 1.32−1.30 (m, 72H, $OC_3H_6C_{12}H_{24}CH_3$), 0.89−0.86 (m, 9H, $OC_{15}H_{30}CH_3$). FABMS: *m*/*z* (% intensity) 963.9 (100, M^+). Calcd for $C_{63}H_{113}NO_5$: 963.86. The product 1-*tert*-butoxycarbonyl-2-(3,4,5-trihexadecyloxyphenyl)pyrrole (300.0 mg, 0.311 mmol) was heated at 190 °C for 15 min. The residue was then chromatographed over flash silica gel column (eluent: CH_2Cl_2/hexane = 2/3) and gave 2-(3,4,5-trihexadecyloxyphenyl)pyrrole as a white solid (260.0 mg, 87%). R_f = 0.27 (CH_2Cl_2/hexane = 2/3). ^{1}H NMR (600 MHz, $CDCl_3$, 20 °C): δ (ppm) 8.34 (br, 1H, NH), 6.84−6.83 (m, 1H, pyrrole-H), 6.64 (s, 2H, Ar-H), 6.41−6.39 (m, 1H, pyrrole-H), 6.28−6.27 (m, 1H, pyrrole-H), 4.00 (t, J = 6.6 Hz, 4H, OCH_2), 3.95 (t, J = 6.6 Hz, 2H, OCH_2), 1.81 (tt, J = 7.2, 6.6 Hz, 4H, OCH_2CH_2), 1.75 (tt, J = 7.2, 6.6 Hz, 2H, OCH_2CH_2), 1.49−1.45 (m, 6H, $OC_2H_4CH_2$), 1.33−1.25 (m, 72H, $OC_3H_6C_{12}H_{24}CH_3$), 0.89−0.86 (m, 9H, $OC_{15}H_{30}CH_3$). FABMS: *m*/*z* (% intensity): 863.9 (41, M^+), 864.7 (100, $M^+ + 1$). Calcd for $C_{58}H_{105}NO_3$: 863.81.

1,3-Bis(5-(3,4,5-trimethoxyphenyl)pyrrol-2-yl)-1,3-propanedione, 4a. A CH_2Cl_2 solution (20 mL) of 2-(3,4,5-trimethoxyphenyl)-pyrrole (145.8 mg, 0.625 mmol) was treated with malonyl chloride (52.9 mg, 0.375 mmol) at room temperature and stirred for 1.5 h at the same temperature. After confirming the consumption of the starting pyrrole by TLC analysis, the mixture was washed with saturated, aq Na_2CO_3 and water, dried over anhydrous $MgSO_4$, filtered, and evaporated to dryness. The residue was then chromatographed over flash silica gel column (eluent: 2% MeOH/CH_2Cl_2) and recrystallized from CH_2Cl_2/hexane to afford the corresponding dipyrrolyldiketone **4a** (104.5 mg, 63%) as a pale-yellow solid. R_f = 0.29 (2% MeOH/CH_2Cl_2). ^{1}H NMR (600 MHz, $CDCl_3$, 20 °C; the diketone is obtained as a mixture of keto and enol tautomers in the ratio of 1:0.34): δ (ppm) keto form 9.48 (br, 2H, NH), 7.16−7.15 (m, 2H, pyrrole-H), 6.75 (s, 4H, Ar-H), 6.54−6.53 (m, 2H, pyrrole-H), 4.26 (s, 2H, CH), 3.95−3.90 (m, 18H, OCH_3); enol form 16.76 (br, 1H, OH), 9.38 (br, 2H, NH), 6.99−6.98 (m, 2H, pyrrole-H), 6.77 (s, 4H, Ar-H), 6.58−6.57 (m, 2H pyrrole-H), 6.38 (s, 1H, CH), 3.89−3.87 (m, 18H, OCH_3). FABMS: *m*/*z* (% intensity): 534.2 (100, M^+), 535.3 (55, $M^+ + 1$). Calcd for $C_{29}H_{30}N_2O_8$: 534.20.

1,3-Bis(5-(3,4,5-trioctyloxyphenyl)pyrrol-2-yl)-1,3-propanedione, 4b. A CH_2Cl_2 solution (20 mL) of 2-(3,4,5-trioctyloxyphenyl)-pyrrole (243.2 mg, 0.444 mmol) was treated with malonyl chloride (37.5 mg, 0.266 mmol) at room temperature and stirred for 1.5 h at the same temperature. After the consumption of the starting pyrrole was confirmed by TLC analysis, the mixture was washed with saturated, aq Na_2CO_3 and water, dried over anhydrous Na_2SO_4, filtered, and evaporated to dryness. The residue was then chromatographed over flash silica gel column (eluent: 1.5% MeOH/CH_2Cl_2) to afford the corresponding dipyrrolyldiketone **4b** (146.3 mg, 59%) as yellowish brown solid. R_f = 0.33 (2% MeOH/CH_2Cl_2). ^{1}H NMR (600 MHz, $CDCl_3$, 20 °C; the diketone is obtained as a mixture of keto and enol tautomers in the ratio of 1:0.34): δ (ppm) keto form 9.41 (br, 2H, NH), 7.14−7.13 (m, 2H, pyrrole-H), 6.71 (s, 4H, Ar-H), 6.50−6.49 (m, 2H, pyrrole-H), 4.23 (s, 2H, CH), 4.04−3.96 (m, 12H, OCH_2), 1.84−1.80 (m, 8H, OCH_2CH_2), 1.77−1.72 (m, 4H, OCH_2CH_2), 1.50−1.47 (m, 12H, $OC_2H_4CH_2$), 1.37−1.28 (m, 48H, $OC_3H_6C_4H_8CH_3$), 0.89−0.87 (m, 18H, $OC_7H_{14}CH_3$); enol form 16.79 (br, 1H, OH), 9.32 (br, 2H, NH), 6.96−6.95 (m, 2H, pyrrole-H), 6.74 (s, 4H, Ar-H), 6.54−6.53 (m, 2H, pyrrole-H), 6.35 (s, 1H, CH), 4.04−3.96 (m, 12H, OCH_2), 1.84−1.80 (m, 8H, OCH_2CH_2), 1.77−1.72 (m, 4H, OCH_2CH_2), 1.50−1.47 (m, 12H, $OC_2H_4CH_2$), 1.37−1.28 (m, 48H, $OC_3H_6C_4H_8CH_3$), 0.89−0.87 (m, 18H, $OC_7H_{14}CH_3$). FABMS: *m*/*z* (% intensity): 1122.9 (100, M^+), 1124.0 (77, $M^+ + 1$). ESI-TOF-MS (% intensity): *m*/*z* 1121.87 (100, $M^- - 1$), 1122.87 (79, M^-). Calcd for $C_{71}H_{114}N_2O_8$: 1122.86.

1,3-Bis(5-(3,4,5-tridodecyloxyphenyl)pyrrol-2-yl)-1,3-propanedione, 4c. A CH_2Cl_2 solution (20 mL) of 2-(3,4,5-tridodecyloxyphenyl)-pyrrole (231.4 mg, 0.33 mmol) was treated with malonyl chloride (28.1 mg, 0.20 mmol) at room temperature and stirred for 1.5 h at the same temperature. After the consumption of the starting pyrrole was confirmed by TLC analysis, the mixture was washed with saturated, aq Na_2CO_3 and water, dried over anhydrous $MgSO_4$, filtered, and evaporated to dryness. The residue was then chromatographed over flash silica gel column (eluent: 1% MeOH/CH_2Cl_2) to afford the corresponding dipyrrolyldiketone **4c** (186.5 mg, 77%) as a pale-yellow solid. R_f = 0.50 (1% MeOH/CH_2Cl_2). ^{1}H NMR (600 MHz, $CDCl_3$, 20 °C; the diketone is obtained as a mixture of keto and enol tautomers in the ratio of 1:0.32): δ (ppm) keto form 9.42 (br, 2H, NH), 7.13−7.12 (m, 2H, pyrrole-H), 6.71 (s, 4H, Ar-H), 6.50−6.49 (m, 2H, pyrrole-H), 4.23 (s, 2H, CH), 4.04−3.96 (m, 12H, OCH_2), 1.84−1.79 (m, 8H, OCH_2CH_2), 1.76−1.72 (m, 4H, OCH_2CH_2), 1.50−1.45 (m, 12H, $OC_2H_4CH_2$), 1.35−1.26 (m, 96H, $OC_3H_6C_8H_{16}CH_3$), 0.89−0.86 (m, 18H, $OC_{11}H_{22}CH_3$); enol form 16.80 (br, 1H, OH), 9.32 (br, 2H, NH), 6.96−6.95 (m, 2H, pyrrole-H), 6.74 (s, 4H, Ar-H), 6.54−6.53 (m, 2H pyrrole-H), 6.35 (s, 1H, CH), 4.04−3.96 (m, 12H, OCH_2), 1.84−1.79 (m, 8H, OCH_2CH_2), 1.76−1.72 (m, 4H, OCH_2CH_2), 1.50−1.45 (m, 12H, $OC_2H_4CH_2$), 1.35−1.26 (m, 96H, $OC_3H_6C_8H_{16}CH_3$), 0.89−0.86 (m, 18H, $OC_{11}H_{22}CH_3$). ESI-TOF-MS (% intensity): *m*/*z* 1458.22 (95, $M^- - 1$), 1459.22 (100, M^-). Calcd for $C_{95}H_{162}N_2O_8$: 1459.23.

1,3-Bis(5-(3,4,5-trihexadecyloxyphenyl)pyrrol-2-yl)-1,3-propanedione, 4d. A CH_2Cl_2 solution (20 mL) of 2-(3,4,5-trihexadecyloxyphenyl)-pyrrole (259.3 mg, 0.30 mmol) was treated with malonyl chloride (25.0 mg, 0.18 mmol) at room temperature and stirred for 1 h at the same temperature. After the consumption of the starting pyrrole was confirmed by TLC analysis, the mixture was washed with saturated, aq Na_2CO_3 and water, dried over anhydrous $MgSO_4$, filtered, and evaporated to dryness. The residue was then chromatographed over flash silica gel column (eluent: 1% MeOH/CH_2Cl_2) and recrystallized from CH_2Cl_2/MeOH to afford the corresponding dipyrrolyldiketone **4d** (155.0 mg, 57%) as a pale-yellow solid. R_f = 0.44 (1% MeOH/CH_2Cl_2). ^{1}H NMR (600 MHz, $CDCl_3$, 20 °C; the diketone is obtained as a mixture of keto and enol tautomers in the ratio of 1:0.32): δ (ppm) keto form 9.40 (br, 2H, NH), 7.13−7.12 (m, 2H, pyrrole-H), 6.71 (s, 4H, Ar-H), 6.50−6.49 (m, 2H, pyrrole-H), 4.23 (s, 2H, CH), 4.04−3.95 (m, 12H, OCH_2), 1.86−1.79 (m, 8H, OCH_2CH_2), 1.77−1.72 (m,

Table 3. Crystallographic Details for Compounds **3a**, **3b**, **3b′**, **3c**, and **5a**

	3a	**3b**	**3b′**	**3c**	**5a**
formula	$C_{23}H_{17}BF_2N_2O_2$	$C_{25}H_{21}BF_2N_2O$	$C_{25}H_{21}BF_2N_2O_2$	$C_{27}H_{25}BF_2N_2O_2 \cdot 0.5CH_2Cl_2$	$C_{29}H_{29}BF_2N_2O_8 \cdot 0.14C_2H_4Cl_2 \cdot 0.20$water
fw	402.20	430.26	430.26	500.78	599.77
crystal size, mm^3	0.30 × 0.20 × 0.10	0.40 × 0.20 × 0.10	0.55 × 0.50 × 0.05	0.55 × 0.30 × 0.10	0.30 × 0.10 × 0.05
crystal system	monoclinic	monoclinic	monoclinic	monoclinic	triclinic
space group	$P2_1/c$ (no. 14)	$P2_1/a$ (no. 14)	$P2_1/c$ (no. 14)	$P2_1/n$ (no. 14)	$P\bar{1}$ (no. 2)
a, Å	11.515(4)	12.443(6)	11.570(8)	14.768(6)	19.008(3)
b, Å	13.020(5)	13.305(5)	13.387(7)	12.991(5)	19.009(4)
c, Å	12.428(4)	25.211(9)	12.969(6)	26.11(1)	28.644(5)
α, (deg)	90	90	90	90	108.952(7)
β, (deg)	98.304(13)	102.175(17)	97.95(2)	101.72(2)	91.954(6)
γ, (deg)	90	90	90	90	96.686(6)
V, Å^3	1843.7(11)	4080(3)	1989(2)	4905(3)	9694(3)
ρ_{calcd}, g·cm^{-3}	1.449	1.401	1.436	1.356	1.438
Z	4	8	4	8	14
T, K	123(2)	123(2)	123(2)	123(2)	293(2)
μ(Mo Kα), mm^{-1}	0.106	0.101	0.103	0.199	0.139
reflns	17854	20152	19074	40940	69380
unique reflns	4207	8451	4550	5721	31257
variables	271	622	290	641	2740
$\lambda_{Mo-K\alpha}$, Å	0.71075	0.71075	0.71075	0.71075	0.71075
R_1 ($I > 2\sigma(I)$)	0.0368	0.0641	0.0773	0.0870	0.1019
wR_2 ($I > 2\sigma(I)$)	0.0906	0.1865	0.2184	0.2129	0.2457
GOF	1.091	1.005	1.072	1.016	1.003

4H OCH_2CH_2), 1.50−1.45 (m, 12H, $OC_2H_4CH_2$), 1.35−1.25 (m, 144H, $OC_3H_6C_{12}H_{24}CH_3$), 0.89−0.86 (m, 18H, $OC_{15}H_{30}CH_3$); enol form 16.77 (br, 1H, OH), 9.32 (br, 2H, NH), 6.96−6.95 (m, 2H, pyrrole-H), 6.73 (s, 4H, Ar-H), 6.54−6.53 (m, 2H pyrrole-H), 6.35 (s, 1H, CH), 4.04−3.95 (m, 12H, OCH_2), 1.86−1.79 (m, 8H, OCH_2CH_2), 1.77−1.72 (m, 4H, OCH_2CH_2), 1.50−1.45 (m, 12H, $OC_2H_4CH_2$), 1.35−1.25 (m, 144H, $OC_3H_6C_{12}H_{24}CH_3$), 0.89−0.86 (m, 18H, $OC_{15}H_{30}CH_3$). ESI-TOF-MS (% intensity): *m*/*z* 1794.58 (65, $M^- - 1$), 1795.58 (100, M^-). Calcd for $C_{119}H_{210}N_2O_8$: 1795.60.

BF_2 Complex of 4a, 5a. To a CH_2Cl_2 solution (30 mL) of **4a** (46.5 mg, 0.087 mmol), was added $BF_3 \cdot OEt_2$ (123.4 mg, 0.87 mmol) and stirred for 10 min at room temperature. After removal of the solvent, flash silica gel column chromatography (eluent: 3% MeOH/CH_2Cl_2) and recrystallization from CH_2Cl_2/hexane afforded **5a** (42.5 mg, 84%) as a red-brown solid. R_f = 0.27 (3% MeOH/CH_2Cl_2). ^{1}H NMR (600 MHz, $CDCl_3$, 20 °C): δ (ppm) 9.60 (br, 2H, NH), 7.22 (dd, J = 2.4, 1.8 Hz, 2H, pyrrole-H), 6.82 (s, 4H, Ar-H), 6.68 (dd, J = 2.4, 1.2 Hz, 2H, pyrrole-H), 3.98 (s, 12H, OCH_3), 3.90 (s, 6H, OCH_3). UV/vis (CH_2Cl_2, λ_{max} [nm] (ϵ, 10^5 M^{-1} cm^{-1})): 515.5 (1.2). FABMS: *m*/*z* (% intensity): 582.2 (100, M^+). Calcd for $C_{29}H_{29}BF_2N_2O_8$: 582.20. This compound was further characterized by X-ray diffraction analysis.

BF_2 Complex of 4b, 5b. To a CH_2Cl_2 solution (30 mL) of **4b** (77.4 mg, 0.069 mmol) was added $BF_3 \cdot OEt_2$ (97.9 mg, 0.69 mmol) and stirred for 10 min at room temperature. After removal of the solvent, flash silica gel column chromatography (eluent: 0.5% MeOH/CH_2Cl_2) and recrystallization from CH_2Cl_2/MeOH afforded **5b** (73.3 mg, 91%) as a red solid. R_f = 0.67 (0.5% MeOH/CH_2Cl_2). ^{1}H NMR (600 MHz, $CDCl_3$, 20 °C): δ (ppm) 9.54 (br, 2H, NH), 7.20 (dd, J = 2.4, 1.8 Hz, 2H, pyrrole-H), 6.79 (s, 4H, Ar-H), 6.65 (dd, J = 2.4, 1.8 Hz, 2H, pyrrole-H), 6.52 (s, 1H, CH), 4.06 (t, J = 6.6 Hz, 8H, OCH_2), 4.00 (t, J = 6.6 Hz, 4H, OCH_2), 1.85 (tt, J = 7.2, 6.6 Hz, 8H, OCH_2CH_2), 1.76 (tt, J = 7.2, 6.6 Hz, 4H, OCH_2CH_2), 1.56−1.47 (m, 12H, $OC_2H_4CH_2$), 1.40−1.29 (m, 48H, $OC_3H_6C_4H_8CH_3$), 0.90−0.88 (m, 18H, $OC_7H_{14}CH_3$). UV/vis (CH_2Cl_2, λ_{max} [nm] (ϵ, 10^5 M^{-1} cm^{-1})): 521.0 (1.2). FABMS: *m*/*z* (% intensity): 1170.6 (100, M^+). ESI-TOF-MS (% intensity): *m*/*z* 1169.84 (100, $M^- - 1$), 1170.84 (73, M^-). Calcd for $C_{71}H_{113}BF_2N_2O_8$: 1170.86.

BF_2 Complex of 4c, 5c. To a CH_2Cl_2 solution (30 mL) of **4c** (123.8 mg, 0.085 mmol) was added $BF_3 \cdot OEt_2$ (120.4 mg, 0.85 mmol) and was stirred for 10 min at room temperature. After removal of the solvent, flash silica gel column chromatography (eluent: CH_2Cl_2) and recrystallization from CH_2Cl_2/MeOH afforded **5c** (121.3 mg, 95%) as a red-brown solid. R_f = 0.78 (CH_2Cl_2). ^{1}H NMR (600 MHz, $CDCl_3$, 20 °C): δ (ppm) 9.54 (br, 2H, NH), 7.19 (dd, J = 2.4, 1.8 Hz, 2H, pyrrole-H), 6.78 (s, 4H, Ar-H), 6.64 (dd, J = 2.4, 1.8 Hz, 2H, pyrrole-H), 6.52 (s, 1H, CH), 4.06 (t, J = 6.6 Hz, 8H, OCH_2), 4.00 (t, J = 6.6 Hz, 4H, OCH_2), 1.86 (tt, J = 7.8, 6.6 Hz, 8H, OCH_2CH_2), 1.76 (tt, J = 7.8, 6.6 Hz, 4H, OCH_2CH_2), 1.53−1.46 (m, 12H, $OC_2H_4CH_2$), 1.38−1.26 (m, 96H, $OC_3H_6C_8H_{16}CH_3$), 0.89−0.87 (m 18H, $OC_{11}H_{22}CH_3$). UV/vis (CH_2Cl_2, λ_{max} [nm] (ϵ, 10^5 M^{-1} cm^{-1})): 521.0 (1.3). ESI-TOF-MS: *m*/*z* (% intensity): 1506.20 (100, $M^- - 1$), 1507.20 (92, M^-). Calcd for $C_{95}H_{161}BF_2N_2O_8$: 1507.23.

BF_2 Complex of 4d, 5d. To a CH_2Cl_2 solution (40 mL) of **4d** (62.5 mg, 0.035 mmol) was added $BF_3 \cdot OEt_2$ (49.7 mg, 0.350 mmol) and was stirred for 10 min at room temperature. After removal of the solvent, flash silica gel column chromatography (eluent: $CHCl_3$) and recrystallization from CH_2Cl_2/MeOH afforded **5d** (59.6 mg, 92%) as a red-brown solid. R_f = 0.78 ($CHCl_3$). ^{1}H NMR (600 MHz, $CDCl_3$, 20 °C): δ (ppm) 9.53 (br, 2H, NH), 7.19 (dd, J = 2.4, 1.8 Hz, 2H, pyrrole-H), 6.78 (s, 4H, Ar-H), 6.64 (dd, J = 2.4, 1.8 Hz, 2H, pyrrole-H), 6.52 (s, 1H, CH), 4.06 (t, J = 6.6 Hz, 8H, OCH_2), 4.00 (t, J = 6.6 Hz, 4H, OCH_2), 1.86 (tt, J = 7.2, 6.6 Hz, 8H, OCH_2CH_2), 1.76 (tt, J = 7.2, 6.6 Hz, 4H, OCH_2CH_2), 1.53−1.46 (m, 12H, $OC_2H_4CH_2$), 1.38−1.26 (m, 144H, $OC_3H_6C_{12}H_{24}CH_3$), 0.89−0.86 (m, 18H, $OC_{15}H_{30}CH_3$). UV/vis (CH_2Cl_2, λ_{max} [nm] (ϵ, 10^5 M^{-1} cm^{-1})): 521.0 (1.2). ESI-TOF-MS: *m*/*z* (% intensity): 1842.55 (89, $M^- - 1$), 1843.55 (100, M^-). Calcd for $C_{119}H_{209}BF_2N_2O_8$: 1843.61.

X-ray Single-Crystal Analysis. Crystallographic data for **3a**, **3b**, **3b′**, **3c**, **5a**, **3a**·TPACl, and **5a**·TBACl are summarized in Tables 3 and 4. A single crystal of **3a** was obtained by vapor diffusion of hexane into a CH_2ClCH_2Cl solution of **3a**. The data crystal was an orange-colored prism of approximate dimensions 0.30 mm × 0.20 mm × 0.10 mm. A single crystal of **3b** was obtained by vapor diffusion of hexane into a CH_2ClCH_2Cl solution of **3b**. The data crystal was an orange-colored prism of approximate dimensions 0.40 mm × 0.20 mm × 0.10 mm. A single crystal of **3b′** was obtained by vapor diffusion of pentane into a CH_2Cl_2 solution of **3b′**. The data crystal was an orange-colored prism of approximate dimensions 0.55 mm × 0.50 mm × 0.05 mm. A single crystal of **3c** was obtained by vapor diffusion of hexane into a CH_2Cl_2 solution of **3c** with a small amount of toluene. The data crystal was a yellow prism of approximate dimensions 0.55 mm × 0.30 mm × 0.10 mm. A single crystal of **5a** was obtained by vapor diffusion of hexane into a CH_2ClCH_2Cl solution of **5a**. The data crystal was a red prism of approximate dimensions 0.30 mm × 0.10 mm × 0.05 mm. A

Table 4. Crystallographic Details for Compounds **3a**·TPACl, and **5a**·TBACl

	3a·TPACl	**5a**·TBACl
formula	$C_{23}H_{17}BF_2N_2O_2$·TPACl·$C_2H_4Cl_2$	$C_{29}H_{29}BF_2N_2O_8$·TBACl·0.5$C_2H_4Cl_2$
fw	722.95	909.74
crystal size, mm^3	0.50 × 0.10 × 0.01	0.40 × 0.20 × 0.10
crystal system	monoclinic	triclinic
space group	$P2_1/n$ (no. 14)	$P\bar{1}$ (no. 2)
a, Å	12.775(4)	12.138(3)
b, Å	8.536(3)	20.055(6)
c, Å	35.084(11)	20.264(5)
α, (deg)	90	85.480(11)
β, (deg)	92.675(11)	78.711(9)
γ, (deg)	90	80.498(10)
V, $Å^3$	3822(2)	4765(2)
ρ_{calcd}, g·cm^{-3}	1.257	1.268
Z	4	4
T, K	123(2)	123(2)
μ(Mo Kα), mm^{-1}	0.285	0.198
reflns	27954	44186
unique reflns	6713	20883
variables	637	1137
$\lambda_{Mo-K\alpha}$, Å	0.71075	0.71075
R_1 ($I > 2\sigma(I)$)	0.0724	0.0816
wR_2 ($I > 2\sigma(I)$)	0.1190	0.1914
GOF	0.856	1.032

single crystal of **3a**·TPACl was obtained by vapor diffusion of hexane into a CH_2ClCH_2Cl solution of the equivalent mixture of **3a** and TPACl. The data crystal was an orange prism of approximate dimensions 0.50 mm × 0.10 mm × 0.01 mm. A single crystal of **5a**·TBACl was obtained by vapor diffusion of hexane into a CH_2ClCH_2Cl solution of the equivalent mixture of **5a** and TBACl. The data crystal was an orange prism of approximate dimensions 0.40 mm × 0.20 mm × 0.10 mm. In each case, data were collected at 123 (**3a**, **3b**, **3c**, **3b′**, **3a**·TPACl, and **5a**·TBACl) or 293 (**5a**) K on a Rigaku RAXIS-RAPID diffractometer with graphite monochromated Mo Kα radiation ($\lambda = 0.71075$ Å), the structure was solved by direct method, and the non-hydrogen atoms were refined anisotropically. The calculations were performed using the Crystal Structure crystallographic software package of Molecular Structure Corporation. CIF files (CCDC-639766-639770, 646480, 639771 for **3a**, **3b**, **3c**, **3b′**, **5a**, **3a**·TPACl, and **5a**·TBACl) can be obtained free of charge from the Cambridge Crystallographic Data Centre via www.ccdc.cam.ac.uk/data_request/cif.

Stopped-Flow Measurements. Stopped-flow measurements were carried out using a Unisoku Stopped-flow Rapid-scan Spectroscopy System RSP-1000.

Atomic Force Microscopy (AFM). AFM measurements were carried out using an SII EPA-400 with an SPI 4000 Probe Station in dynamic force mode (tapping mode).

Scanning Electron Microscopy (SEM). SEM images were obtained with a HITACHI S-4800 scanning electron microscope at acceleration voltages of 15 kV. A gold-coated quartz plate as well as silicon (100) was used as substrate, and a platinum coating was applied using a HITACHI E-1030 ion sputterer.

X-ray Diffraction Analysis (XRD). XRD measurements were examined using a RIGAKU RINT Ultima III X-ray diffractometer. Octane gels of **5d** were dropped on a glass plate for XRD, left to dry at 60 °C under high vacuum, and aged at 5 °C for 12 h, and the observations were performed at room temperature.

DFT Calculations. Ab initio calculations of **3a**−**c** and their F^- and Cl^- binding complexes were carried out by using Gaussian 03 program[22] and an HP Compaq dc5100 SFF computer. The structures were optimized, and the total electronic energies were calculated at the B3LYP level using a 6-31G** basis set for receptors and [1+1] anion complexes.

Acknowledgment. This work was supported by Grant-in-Aid for Young Scientists (B) (No. 17750137) and Scientific Research in a Priority Area "Super-Hierarchical Structures" (No. 18039038, 19022036) from the Ministry of Education, Culture, Sports, Science and Technology (MEXT), Nissan Science Foundation, and the "Academic Frontier" Project for Private Universities, namely the matching fund subsidy from the MEXT, 2003−2008. We thank Prof. Atsuhiro Osuka, Mr. Shigeki Mori, and Mr. Shohei Saito, Kyoto University, for X-ray analyses, Prof. Hiroshi Shinokubo and Mr. Masatoshi Mizumura, Kyoto University, for ESI-TOF-MS measurements, Dr. Tomohiro Miyatake, Ryukoku University, for FAB-MS measurements, Prof. Takashi Hayashi and Dr. Takashi Matsuo, Osaka University, for stopped-flow measurements, Prof. Tadashi Mizoguchi, Dr. Michio Kunieda, Ritsumeikan University, for ^{1}H DOSY measurement, and Prof. Hitoshi Tamiaki, Ritsumeikan University, and Dr. Jonathan P. Hill, NIMS, for helpful discussions.

Supporting Information Available: Anion binding behaviors (spectral changes and optimized structures) of C_3-bridged oligopyrrole derivatives, characteristic properties of supramolecular organogel formation, CIF files for the X-ray structural analysis of **3a**−**c**, **3b′**, **5a**, **3a**·TPACl, and **5a**·TBACl, and complete ref 22. This material is available free of charge via the Internet at http://pubs.acs.org.

JA074435Z